



School of Chemistry

# Investigating the Doping of Diamond with Magnesium

Louisa Gryspeerdt

**April 2014**

Supervisor: Professor P.W. May

Second Assessor: Dr N.A. Fox

**Submitted in partial fulfilment of  
the requirements for the  
Honours degree of MSci in  
Chemistry**

## Abstract

Finding a suitable shallow donor to produce n-type semiconducting diamond with numerous electronic applications and with potential as a thermionically emitting material has proved challenging. Following attempts with lithium, magnesium seems a strong candidate. Incorporation of magnesium into CVD diamond was achieved by an in-diffusion method by depositing a suspension of magnesium nitride in chloroform with polymer onto a pre-grown diamond film and allowing diffusion in a hydrogen atmosphere for one hour at approximately 800°C. The pre-grown diamond films were either nitrogen-doped (using ammonia) or boron-doped (using diborane) and grown for 4 hours using hot filament chemical vapour deposition method.

The presence of magnesium was found to affect the morphology of the films producing 'roughened' facets (Scanning Electron Microscopy, SEM). Energy-dispersive X-ray spectroscopy (EDX) was also used to characterise the films and indicated the presence of magnesium. This qualitative technique suffered a number of limitations so Secondary Ion Mass Spectrometry (SIMS) was also performed. SIMS was used to produce depth profiles of the films, detecting secondary magnesium and magnesium oxide ions. The magnesium diffused  $\pm 200$  nm although possibly aided by magnesium residing in the grain boundaries. Results do not indicate the nature of the magnesium in the diamond film (whether residing on substitutional sites or interstitial sites or whether within the grain boundaries).

The flow rates of the ammonia and diborane were varied and found to affect the morphology of the films which was analysed using SEM. It was found that for ammonia, a high flow rate of 0.75 sccm was too high to permit effective magnesium incorporation and so 0.2 sccm was preferred. However, all flow rates of diborane tested were suitable.

Conductivity of the films was measured. Samples where magnesium was diffused into a nitrogen-doped film were found to have a high resistivity, greater than 20 M $\Omega$ . Boron-doped diamond films are known to be conductive and thus have a much lower resistivity, although when magnesium was diffused the resistivity increased. When comparing high and low doped magnesium films, the higher magnesium content has a lower resistance.

The presence of magnesium alters the behaviour of the diamond film and it should be considered as a useful dopant in diamond.

## Contents

Abstract.....	1
Contents .....	2
Chapter 1 Introduction .....	4
1.1 Introduction to diamond.....	4
1.2 High pressure high temperature diamond .....	5
1.3 Chemical vapour deposition.....	7
1.3.1 Introduction to chemical vapour deposition.....	7
1.3.2 Use of hot filaments .....	7
1.3.3 Use of plasmas .....	8
1.3.4 Substrate.....	9
1.3.5 Mechanism of diamond growth .....	10
1.3.6 Importance of hydrogen gas.....	11
1.3.7 Epitaxy, structure and film quality.....	12
1.4 Introduction to diamond as a semiconductor .....	12
1.5 Acceptors in diamond and p-type semiconductivity .....	13
1.6 Donors in diamond and n-type semiconductivity .....	14
1.7 Methods of doping .....	19
1.8 Applications .....	20
Chapter 2 Experimental Methods .....	25
2.1 Hot Filament reactor .....	25
2.2 Magnesium nitride suspension.....	26
2.3 The diffusion process .....	28
2.4 Scanning electron microscopy .....	29
2.5 Secondary ion mass spectrometry .....	30
2.6 Energy-dispersive X-ray spectroscopy .....	33
2.7 Conductivity measurements.....	34
Chapter 3 Results and Discussion.....	35
3.1 Scanning Electron Microscopy (SEM) .....	35
3.2 Secondary Ion Mass Spectrometry (SIMS) .....	38
3.3 Energy-Dispersive X-Ray Spectroscopy (EDX).....	43
3.4 Conductivity Measurements .....	46
Chapter 4 Conclusion.....	49
Chapter 5 Future Work .....	51

5.1 X-Ray photoelectron spectroscopy (XPS) .....	51
5.2 Role of the grain boundaries .....	51
5.3 Diffusion conditions.....	51
5.4 Film quality .....	52
5.5 Test for thermionic emission.....	52
5.6 Computational studies.....	52
Chapter 6 Acknowledgements .....	53
Chapter 7 Bibliography .....	54
Chapter 8 Appendix .....	58

# Chapter 1 Introduction

## 1.1 Introduction to diamond

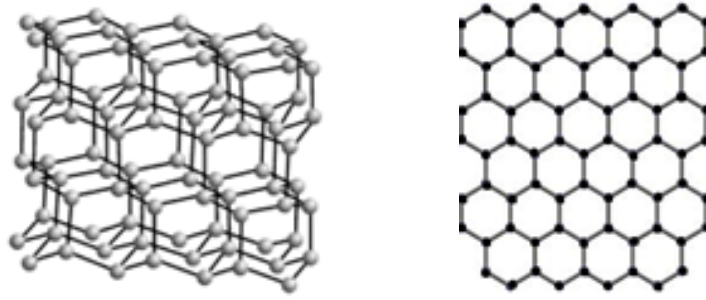
Diamond has attracted attention for many years. Whilst many have been drawn to it for its aesthetic qualities, diamond has proved of great scientific interest owing to its superlative properties and use as a potential material for a wide range of applications [1].

Table 1.1 summarises the properties of diamond. Diamond is recognised for its extreme strength, indeed it is the hardest known material and the least compressible as well as having the highest thermal conductivity. Diamond is an electrical insulator at room temperature with a wide band gap of 5.4 eV but by incorporating impurities, a process known as doping, it is possible to obtain semiconducting diamond.

Mechanical hardness	~ 90 GPa
High Bulk modulus	$1.2 \times 10^{12} \text{ N m}^{-2}$
Low compressibility	$8.3 \times 10^{-13} \text{ m}^2 \text{ N}^{-1}$
High thermal conductivity	$2 \times 10^3 \text{ W m}^{-1} \text{ K}^{-1}$
Electrically insulator – RT resistance	$\sim 10^{13} - 10^{16} \Omega \text{ cm}$
Wide band gap	5.4 eV
Broad optical transparency	UV – far IR (~40 $\mu\text{m}$ )
Chemically inert	
High radiation hardness	

**Table 1.1.** Properties of diamond [1].

Diamond is one of the natural allotropes of carbon, the other being graphite [2]. Graphite is a network of carbon atoms,  $sp^2$  bonded and forming layers between which are delocalised electrons, whereas diamond forms a tetrahedral lattice of  $sp^3$  bonded carbon atoms (structures shown in Figure 1.1). Diamond has a longer carbon-carbon bond length than graphite.



**Figure 1.1** Structures of carbon allotropes: diamond (left) [3] and graphite (right) [4].

Despite the tremendous stability of diamond, it is in fact graphite which is the more thermodynamically stable form of carbon at room temperature and pressure [2]. Figure 1.2 shows the energy diagram of graphite and diamond. Surprisingly the activation barrier for the conversion of graphite to diamond is  $728 \pm 50 \text{ kJ mol}^{-1}$  yet the standard enthalpies of these carbon forms are only separated by a mere  $2.9 \text{ kJ mol}^{-1}$  [5]. It is the existence of this large activation barrier which defines diamond as a rare, metastable form of carbon, possessing kinetic but not thermodynamic stability [1].

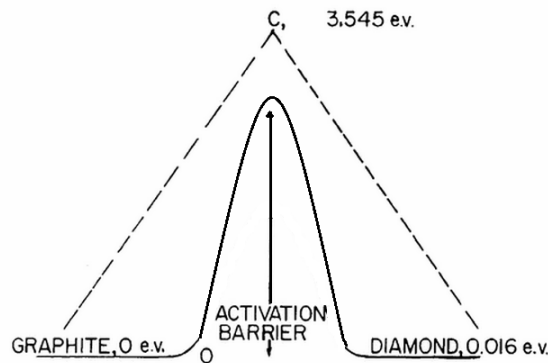


**Figure 1.2.** Energy diagram of carbon and graphite (figure not to scale, adapted from source) [6].

## 1.2 High pressure high temperature diamond

The desire for diamond, for use in scientific applications, is compromised by its scarcity and cost [1]. This has led to much investigation into the possible synthesis of diamond. The first synthesis of diamond was the conversion of graphitic carbon to diamond under high pressure and high

temperature (HPHT) using a hydraulic press which exerted up to 1000 tons [7]. Such conditions are needed where diamond is the stable form of carbon and are based upon how diamond is naturally formed within the Earth. The phase diagram (Figure 1.3) illustrates this, showing the stable form under varying temperature and pressure. Being more dense than graphite,  $3.51 \text{ g mol}^{-1}$  compared to  $2.25 \text{ g mol}^{-1}$ , diamond is the more stable form at high pressure [8]. High temperature is also needed to overcome the activation barrier and hence the extreme conditions for this diamond synthesis.

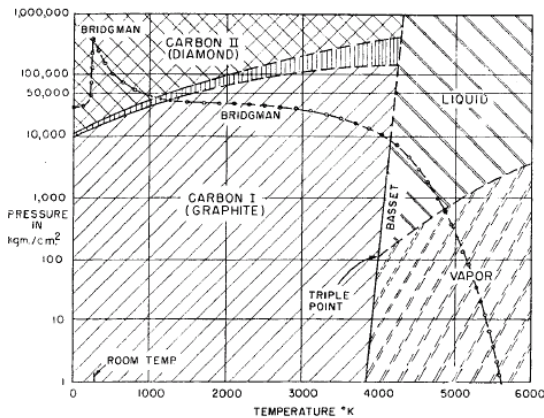


**Figure 1.3.** Carbon phase diagram [7].

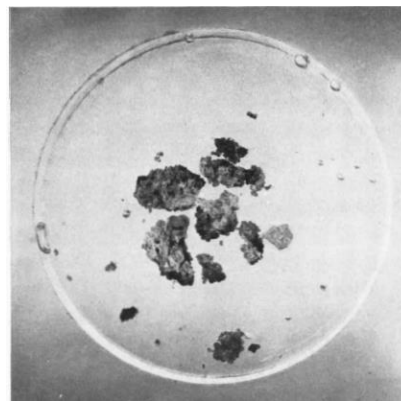


**Figure 1.4.** General Electric's diamond crystals [8].

The apparatus required to perform this procedure proved an engineering challenge. Originally, vessels were designed which could withstand pressures of  $50,000 \text{ kg cm}^{-3}$  but combined with hot temperatures the materials would be weakened and fail. Later, equipment was able to support  $100,000 \text{ kg cm}^{-3}$  and 2300 K and this could be sustained for hours at a time [7]

The HPHT technique for synthetic diamonds is limited by expensive apparatus [9]. It also suffers from a limitation on the form and size of crystals which are obtained [1] [10].

## 1.3 Chemical vapour deposition

### 1.3.1 Introduction to chemical vapour deposition

Chemical vapour deposition (CVD) is an alternative method of synthesising diamond which operates at conditions under which diamond is metastable. It is by this method that it has become possible to synthesise diamond under low pressure [11]. These methods involve the activation of precursor gases such as methane and hydrogen [12]. This generates the carbon-containing radicals and reactive hydrogen atoms which can react and adsorb to a substrate surface, eventually resulting in the formation of diamond [1] [12]. The mechanism of this is discussed in detail in section 1.3.5.

There are several different methods of CVD of diamond. The main difference between these is the way in which the precursor gases are activated – this may be done by hot filaments or plasmas.

### 1.3.2 Use of hot filaments

Hot filament CVD (HFCVD) was the first successful low pressure synthesis of diamond on non-diamond substrates [13].

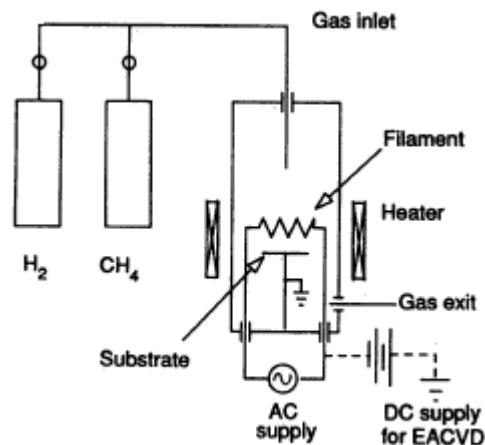


**Figure 1.5.** Schematic diagram of the apparatus used for HFCVD [11].

A number of different filaments have been used in this process for example tungsten, tantalum and rhenium [14].

The controlling parameters in this method are the filament temperature, substrate geometry and distance between the filament and substrate. All affect the number of activated particles which reach the surface [15].

The optimum distance between filament and substrate requires a deal of compromise: a larger distance leads to generation of a more uniform diamond film however, if the distance is reduced, more activated particles (movement of which is controlled by diffusion) will be able to reach the surface and increase the growth rate [16]. In general, the growth rate will be increased by increasing filament temperature which is normally around 2000 °C [17].

The principle advantage of HFCVD over other CVD methods is that it requires comparatively cheap apparatus [15]. However there are a number of disadvantages of HFCVD as it suffers from a slow growth rate, normally in the region of 1µm per hour [15]. The filaments also have a limited lifetime due to their possible carburization whereby methane molecules adsorb on the surface, decompose and diffuse through the metal. Carbides are brittle and therefore the filaments can easily break [14]. Carbide formation can be encouraged by higher temperatures and some metals may be more resistant than others - tantalum is more resistant than tungsten [18], however, rhenium, although much more expensive, may be preferable as it does not form a carbide [14]. Additionally, the diamond film may be contaminated by the metal filament [1].

### 1.3.3 Use of plasmas

This method employs plasmas to transform the reagents in the plasma stream into reactive atoms and ions [19]. The most common type is microwave CVD (MWCVD) [1] which is illustrated below. This method has the advantage of increased growth rate, in excess of 10µm/hour [20]. As well as this, with no filament, there is no contamination of the diamond film [1]. However, smaller substrates are used resulting in a reduced film quality compared to those grown with HFCVD [5].

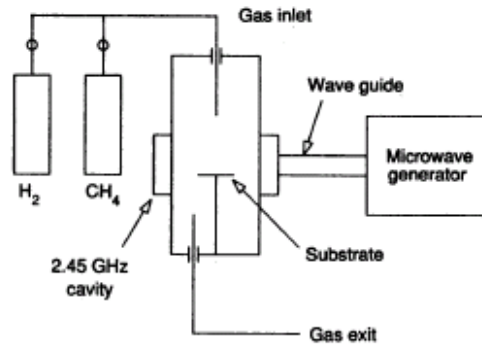


**Figure 1.6.** Schematic diagram of the apparatus used for MWCVD [11].

An alternative is generation of a plasma jet by a dc current which has produced the highest growth rate for CVD of diamond - 930  $\mu\text{m}/\text{hour}$  [21]. However, this is only achieved over very small areas.

### 1.3.4 Substrate

There are a number of requirements for the substrate: it must have a high melting point in order to withstand the conditions for diamond growth; it must have a similar thermal expansion coefficient to diamond so that during extreme heating and cooling the diamond does not crack; and it must be able to form a carbide layer so that the diamond film can adhere to the substrate. The carbide layer should not be too thick or there could be a delayed start to diamond growth [1].

An important consideration is the temperature of the substrate as can be seen in Figure 1.7. The growth increases with substrate temperature up until around 950  $^{\circ}\text{C}$ . In HFCVD the temperature can be difficult to control and the temperature gradient between the filament and substrate needs to be taken into account [22]. In MWCVD the substrate temperature can be altered by adjusting the microwave power.

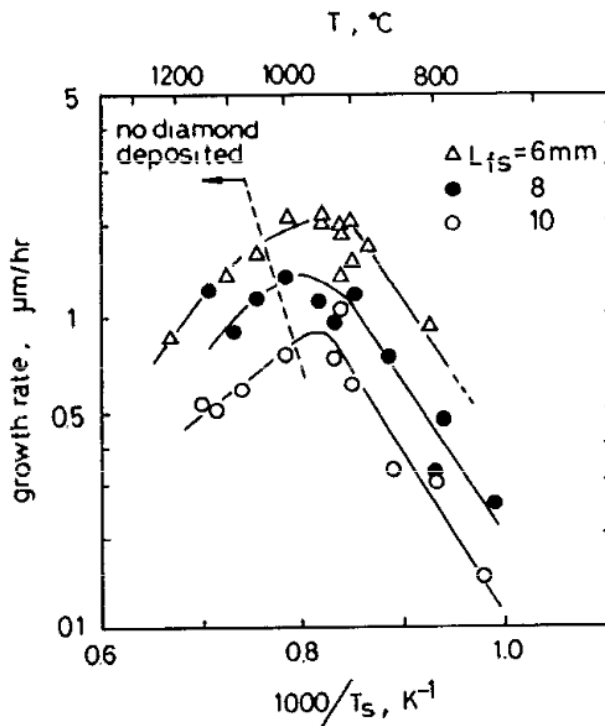


**Figure 1.7.** Graph showing the dependence of growth rate upon substrate temperature. p-type silicon used as the substrate [23].

### 1.3.5 Mechanism of diamond growth

The atoms in the gas phase move by convective and diffusive flow [5]. Figure 1.5 shows the setup of the gases with respect to the apparatus in a hot filament reactor. Firstly the precursor gases enter the chamber and are transported towards the filament around which free radicals and ions are generated. There are radicals and ions in the region between the substrate and the filament and these can adsorb onto the substrate surface [5] [1].

The first step in the mechanism for diamond growth is the creation of an active site on the substrate surface by loss of a hydrogen atom. This site will then be rapidly attacked by, most commonly another hydrogen atom, restoring its original form, but sometimes a carbon radical. The probability of this carbon radical attack is not favourable; the ratio of hydrogen to carbon radicals is 50 to 1. However, it still occurs and this same process of active site generation and carbon adsorption may occur on an adjacent site, and then further hydrogen abstraction on one of these chemisorbed carbon atoms will generate a radical. This radical can then attack one of the other nearby chemisorbed carbon atoms forming a ring structure [1]. The process is outlined below.

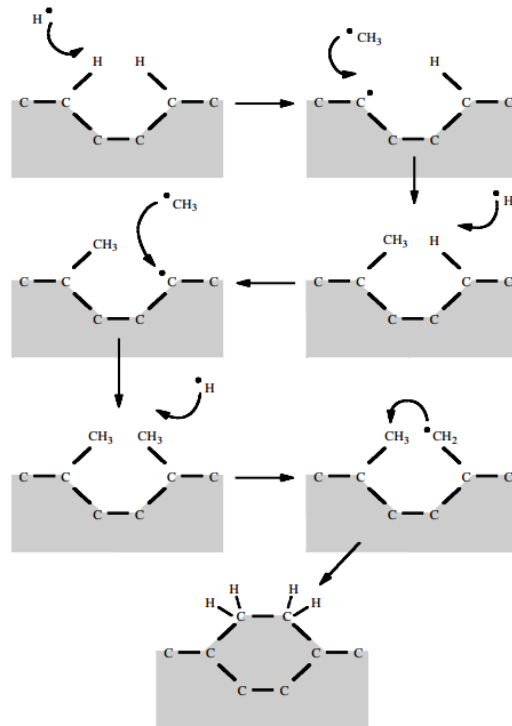
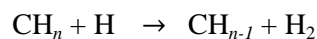


**Figure 1.8.** A schematic diagram of the reaction process occurring at the diamond surface leading to stepwise addition of  $\text{CH}_3$  species and diamond growth [1].

### 1.3.6 Importance of hydrogen gas

Without hydrogen gas, diamond growth would not be possible. The presence of hydrogen is imperative for a number of reasons:

- 1) Reducing the critical radius for diamond nucleation. Without hydrogen, a diamond substrate is necessary but with hydrogen, diamond crystals nucleate readily and are subsequently covered by hydrogen, reducing the surface energy and thus the critical radius [6]
- 2) Generating carbon-containing radicals [6]. The general equation



Where  $\text{CH}_n$  is a hydrocarbon radical species resulting from the reaction of stable hydrocarbon species with H atoms [24].

- 3) Surface termination to remove ‘dangling bonds’. This process was first identified by low energy, high resolution electron energy loss spectroscopy identifying the vibrational modes of hydrogen [25].

The processes are driven by the strength of the hydrogen-hydrogen bond. The carbon-carbon bond is weaker than a carbon-hydrogen bond so the hydrogen abstraction to generate a carbon-carbon bond is thermodynamically unfavourable and unlikely to occur unless hydrogen is present which introduces stronger hydrogen-hydrogen bond formation as a driving force [1].

There are other possibilities instead of using hydrogen gas. Indeed oxygen has been used and produced diamond films with an improved quality [26]. It is found that with the addition of oxygen, the deposition of graphitic and amorphous carbon is suppressed as well as the diamond growth rate being increased [27].

Other suggestions have been made to use fullerenes instead of even hydrogen or oxygen potentially avoiding defects incurred by an inevitable degree of hydrogen incorporation. This alternative method was originally thought to proceed via  $C_2$  however this has since been disproved [28].

### 1.3.7 Epitaxy, structure and film quality

The quality of the diamond film formed is important: for semiconductor purposes an atomically flat surface, low defect density and low level of residual impurities is needed [29].

This quality can be a challenge to obtain. Homoepitaxial growth has been successful for semiconductor use but heteroepitaxial growth (for instance on silicon) is more difficult owing to the lattice mismatch [30].

For films grown with high methane concentrations, the film quality is influenced by nitrogen. With no nitrogen the quality is much poorer – the film is fine grained and lacking crystallinity at the surface. However, above 1% nitrogen, the concentration is too high and quality deteriorates. When growing with low methane concentrations, however, the same effect was not observed [31].

## 1.4 Introduction to diamond as a semiconductor

There are a number of useful properties of diamond which make it an attractive choice for a semiconductor.

- Diamond possesses a high break down voltage, high saturation velocity and high thermal conductivity making it ideal for high frequency, high power devices [32]

- Diamond has a very high electron velocity at high electric field as well as high hole mobility, high dielectric strength and low dielectric constant [33]
- Semiconducting diamond may be obtained by doping with impurities [34]

Applications are currently somewhat limited by the ability to successfully dope diamond, in particular, to produce n-type conducting diamond [35].

## 1.5 Acceptors in diamond and p-type semiconductivity

In order to create p-type semiconducting diamond, acceptors are used. Boron is found as an impurity in natural diamond [36] and is the dominant impurity in type IIb diamonds. These are rare diamonds containing a concentration of less than 1ppm of boron [37]. Semiconducting diamonds have been synthesised with the addition of boron to make them p-type, reaching resistivity as low as  $10^3$  ohm cm [38].

The conductivity increases with increased amount of doping. In low-dose samples, natural impurities and defects may compensate the activity of boron acceptors [39]. Another factor is the dependence of activation energy of hole conduction upon boron concentration – the activation energy decreases with increasing boron content, reportedly vanishing at boron content greater than  $10^{20}$  cm<sup>-3</sup> and resulting in a metal-insulator transition [40].

Boron normally adopts substitutional sites in the diamond lattice and boron complexes and interstitials are unlikely to occur as the formation energy is larger than for substitutional boron [41].

A high boron content ( $3.9 \times 10^{18}$  cm<sup>-3</sup>) can be achieved with a high Hall mobility ( $585$  cm<sup>2</sup>/(Vs)) by boron ion implantation and annealing to  $1450$  °C [42]. Other methods for boron-doping are possible, typically using diborane gas [43] [44].

Aluminium has been considered as an acceptor in diamond but this possibility has been ruled out. Experiments found the concentration of aluminium, measured by slow neutron activation analysis, is lower than the concentration of acceptor centres and therefore it cannot be acting as an acceptor [45] and so boron has remained the principle dopant for producing p-type diamond [46].

## 1.6 Donors in diamond and n-type semiconductority

### 1.6.1 Nitrogen

Nitrogen is a very common natural impurity in diamond: approximately 98% of all clear, naturally occurring diamonds are type I, that is, contain nitrogen [47]. Nitrogen normally resides in diamond at substitutional sites [48] by using its 5 valence electrons to form 3 bonds and a lone pair [49]. It is expected that nitrogen would be a donor in diamond as it has an excess of electrons however nitrogen is found to be a deep donor [50] with an ionization energy in diamond of  $1.62 \pm 0.02$  eV [51] and an energy level of 1.7 eV below the conduction band [52]. The deep donor nature of nitrogen makes it generally undesirable as a donor in diamond despite the practical advantages of nitrogen being highly soluble in diamond and having a low formation energy of -0.4 eV [49].

The reason for nitrogen being a deep donor in diamond is the distortion which occurs within the lattice as can be seen in Figure 1.9 which results in the nitrogen-carbon bond length being 28% longer than the carbon-carbon bond length.

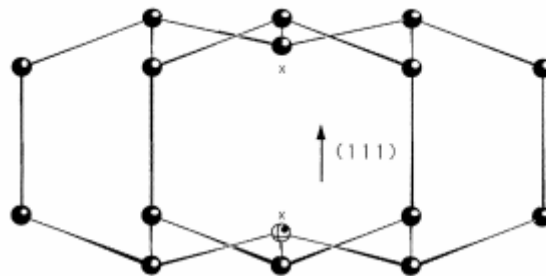


**Figure 1.9.** The relaxation around the substitutional nitrogen in diamond. The white atom represents the nitrogen atom which moves from its unrelaxed position  $x$ . The carbon atom (black atom) moves in the same direction from its original position, also  $x$  [49].

The single electron on the carbon, called a ‘dangling bond’, repels the lone pair on the nitrogen causing a lengthening of the bond. The carbon migrates further from its original position than the nitrogen [49]. The distortion is longer than predicted by Jahn Teller effect [53].

Nitrogen has other effects on the properties of the diamond. It is found that an increased nitrogen concentration reduces the amount of surface deterioration, increases growth rate and results in fewer point defects such as carbon vacancies [54]. The influence of vacancies on the relative stabilization of diamond over graphite has been identified: the formation energy of vacancies in diamond is lower than that in graphite and the formation energy of vacancies in diamond can be changed by varying the Fermi level in diamond which cannot be done in metallic graphite [55].

### 1.6.2 Phosphorus

Phosphorus has been considered as an alternative potential donor in diamond as it has been successfully used to dope and create n-type silicon, analogous to diamond [56] [57]. The first success with phosphorus implantation into diamond was with the use of phosphine gas yielding an activation energy of 0.43 eV and a Hall mobility of 23 cm<sup>2</sup>/(V s) at 500 K [58]. A change in the MWCVD system used for growth, resulted in n-type phosphorus-doped films with a carrier activation energy of approximately 0.6eV. The carrier mobility was around 100 cm<sup>2</sup>/(V s) and the resistance was typically on the order of 10<sup>5</sup> Ω. Infrared spectroscopy has indicated that phosphorus in the diamond lattice is neutral and occupies substitutional sites [59]. However there are a number of disadvantages for using phosphorus as a dopant in diamond: resistivity of phosphorous-doped films may be too high for practical use [60]; annealing at high temperatures can lead to deactivation [61]; and it is thought not suitable for obtaining high quality diamond films [50].

### 1.6.3 Lithium and Sodium

Lithium and sodium are interstitial donors and predicted to be shallow donors [49] [62]. In order for a donor to be a shallow donor it must be in a higher energy state inside the diamond than when outside, making it thus unlikely to be incorporated in the lattice unless driven by large non-equilibrium events [63]. In the case of lithium, it has been found that a number of the lithium atoms occupy substitutional sites as acceptors which can compensate the interstitial sites and increase the resistivity [64] [62].

The formation energies of lithium and sodium in diamond are relatively high, 5.5 eV and 15.3 eV, respectively (sodium being greater because of the larger size of its atom), which causes small equilibrium solubilities and thus doping can be a challenge [49]. The high formation energy of the

interstitials is due to the potential energy experienced by the atoms resulting from the stiffness of the carbon lattice which causes large relaxations around defects and a large band gap and high electron density in diamond [65].

Lithium has a low activation energy in diamond 0.85 eV [49], elsewhere stated even lower 0.26 eV [66]. Sodium being a larger atom has a larger activation energy (3.5 eV) in diamond [67]. Lithium is quite mobile in diamond with a diffusion coefficient in the range  $10^{-15}$  to  $10^{-14}$  cm<sup>2</sup>/s at 400 – 860 °C [66] which can lead to some problems. For example, upon annealing, lithium can diffuse readily and it is possible it will remain trapped at substitutional sites or lithium may aggregate into electrically inactive clusters [68]. Figure 1.10 shows the increase in resistance of doped films with temperature.

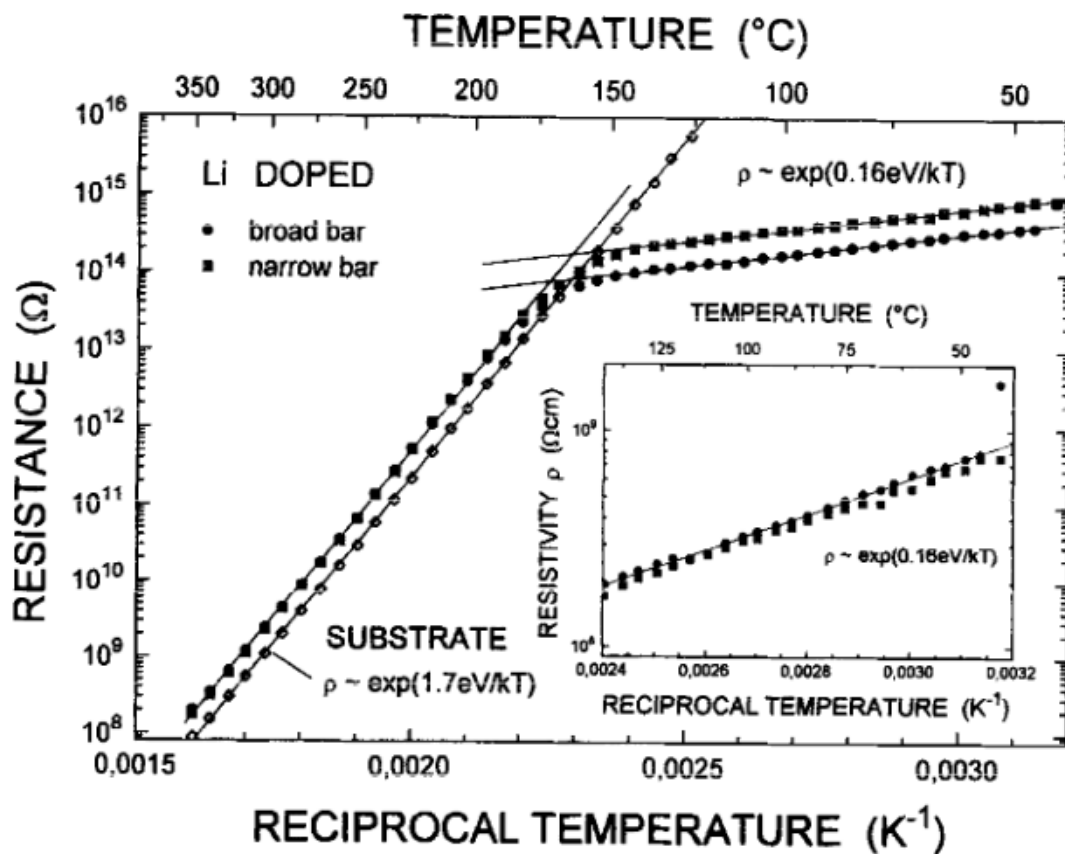


**Figure 1.10.** Electrical resistance and electrical conductivity of a 300 nm thick lithium-doped homoepitaxial layer [69].

The problem of lithium diffusing into clusters has been prevented by successfully incorporating lithium into diamond by co-doping with nitrogen [68]. The nitrogen ‘traps’ the lithium and reduces its mobility. Ammonia is used as the source of nitrogen and is preferable over nitrogen gas as it results in a much greater amount of nitrogen incorporation (experiments were carried out in a hot filament reactor and with insufficient energy to break strong nitrogen-nitrogen triple

bonds in  $N_2$  molecules). Lithium nitride was used as a source of lithium and the doping was carried out using an in-diffusion method, avoiding damage incurred with other techniques such as ion implantation (discussed further in section 1.7 Methods of doping). Secondary ion mass spectrometry (SIMS) was used to analyse the composition of the films. Figure 1.11 shows the SIMS results and indicate that lithium was incorporated into the film with a peak at around 200 nm. The peak is broadened  $\pm 100$  nm as the lithium has diffused either side.

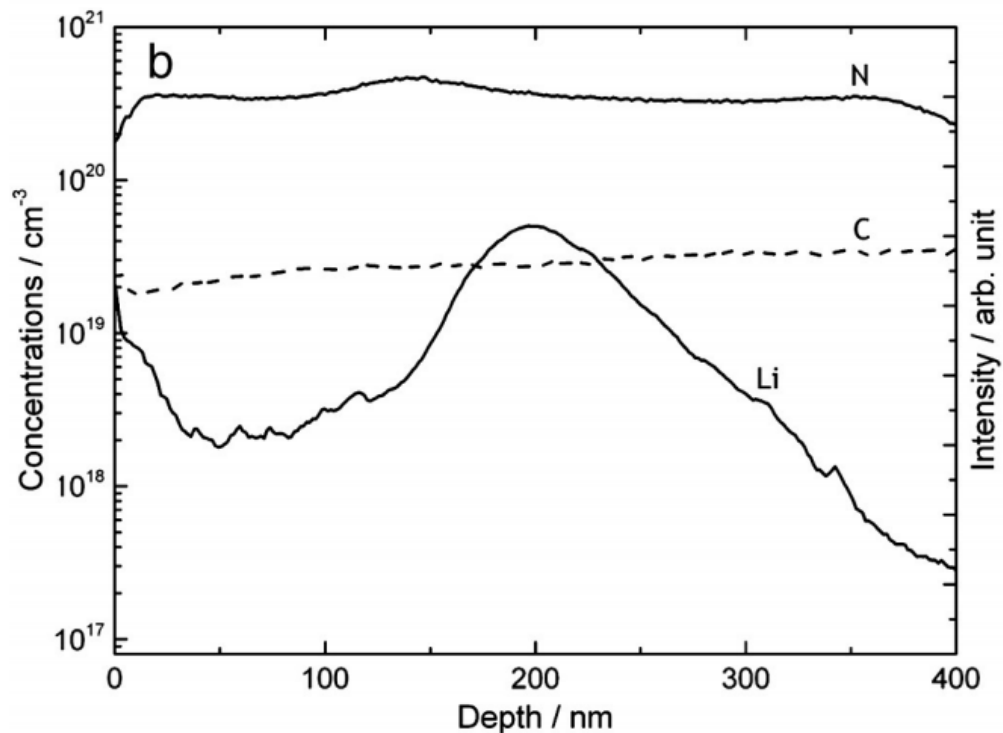


**Figure 1.11.** SIMS depth profile of Li/N co-doped diamond film.  $Li_3N$  added after film thickness was  $\sim 2\mu m$ . Left hand axis shows concentrations of Li and N whilst right hand axis shows C intensity [68].

With sodium, there is a problem in that it is favourably substitutional in diamond and therefore, not an n-type donor. Sodium is 8.73 eV more stable when interstitial is trapped at a vacancy and the formation energy of a vacancy in diamond is 5.86 eV so substitutional formation energy is 2.87 eV lower than interstitial formation energy [67].

### 1.6.4 Sulfur and oxygen

Group 6 elements are another possibility for n-type donors. Small amounts of  $H_2S$  have been found to create a negative Hall coefficient for diamond films, indicative of n-type behaviour. This addition was also found to improve the crystal quality (smooth surface) when the film is deposited under conditions of 50-60 ppm  $H_2S$  but crystal quality decreased when 60 ppm was exceeded [60]. Unfortunately it was later found that these results were due to boron contamination and actually p-type diamond had been produced. The graph below shows that the data for the sulfur-doped samples is indistinguishable from that of boron-doped. Boron contamination was also confirmed by SIMS [61].

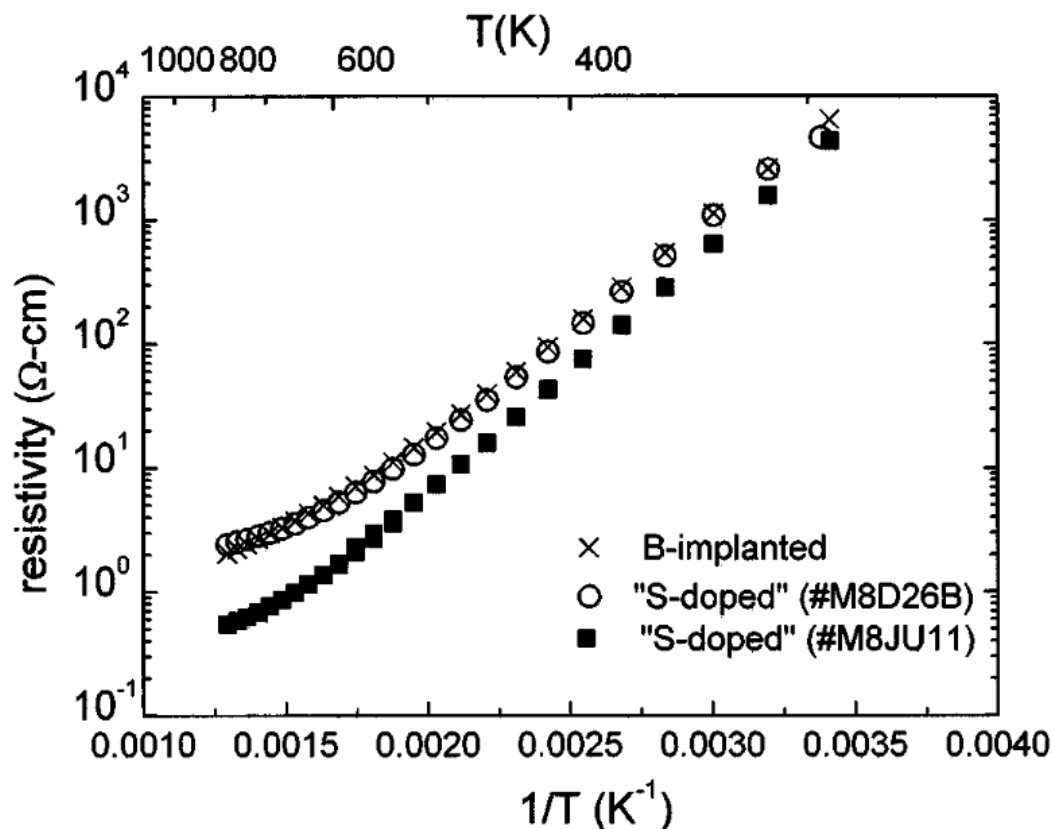


**Figure 1.12.** Measured resistivity as a function of inverse temperature for a boron-doped homoepitaxial diamond layer and two sulfur-doped layers [61].

Sulfur is mostly ionized in the doubly charged state as this has the lowest formation energy but this is not a donor. Neutral sulfur and singly charged sulfur may result from ionization and although these are shallow donors, they are not present in great enough abundance [70].

It has been suggested that injecting oxygen gas during CVD to dope with O could produce n-type diamond: the energy level of oxygen is 0.32 eV below the conduction band. The oxygen atoms would need to occupy substitutional sites with high formation energies in order to act as donors. [63].

## 1.7 Methods of doping

### 1.7.1 In-diffusion

Doping via diffusion is mostly used for impurities which have a small energy of formation [71]. A major advantage is that this method does not damage the sample; no defects are introduced aside from the impurity [72] [73]. Attempts have been made to use this technique to dope diamond with lithium [74] [68]. Other studies have stated that the solubility of lithium (and sodium) are too low for this technique [71]. Indeed the low solubility of lithium in diamond may result in a gradient in the concentration of lithium through the diamond film, with higher levels of the dopant at the surface and the conductivity of the sample is little improved [75]. Other studies have shown a higher conductivity achieved with diffusion with the aid of applying an electric field [72]. It has also been discussed that lithium diffuses well through the grain boundaries of polycrystalline diamond [72] [73]. However, in-diffusion does not create a uniformly doped sample.

### 1.7.2 Ion implantation

This method has successfully been used to dope diamond with boron [36], phosphorus [76] and lithium [74]. It is important to recognise that defects are introduced by this method, such as vacancies, vacancies and interstitials and their combinations, which may have an effect on conductivity [72]. Indeed, the literature is somewhat conflicting upon the origins of conductivity in diamond films doped by this method. It is argued by some that conductivity is caused by the damage incurred by this method and not by the impurities themselves [74]. Others provide evidence that it is not the damage alone that is causing conductivity as there is no electrical conductivity observed when inert ions are implanted [76] [77].

### 1.7.3 Kinetic trapping

This is the favoured method when the energy of formation of the impurity in the diamond is low. The formation energy of the impurity is defined as the energy of the impurity in diamond compared to the bulk impurity and bulk diamond [71]. For example boron, which has a negative formation energy of - 0.5 eV, is normally incorporated during growth using diborane as a precursor gas and p-type behaviour of the resulting films has been observed [71]. As boron doping level increases ( $\sim 10^{17}$  to  $10^{19}$  cm<sup>-3</sup>), the activation energy of electrical conductivity was found to decrease (from 0.37 eV to 0.1 eV) [78]. Phosphorus has been incorporated using phosphine, although much less successfully than boron incorporation with diborane [79], but nevertheless has been found to demonstrate n-type behaviour [80].

## 1.8 Applications

### 1.8.1 Electrodes

Semiconducting diamond has electrochemical potential as an electrode, particularly useful because of its inert surface and chemical resistance, making it suitable for harsh environments [81]. Examples of use of these electrodes include boron-doped diamond electrodes in hydrogen and oxygen evolution [82] and reduction of nitrile and nitrate to ammonia – a difficult process aided by the slow release of hydrogen from cathodically polarised diamond electrodes [83].

### 1.8.2 Light emitting diodes (LEDs)

In order to create an LED, a p-n junction is required. The basic working principle is that electrons (from the n-type semiconductor) and holes (from the p-type semiconductor) can recombine, releasing energy in the form of photons. This energy corresponds to the band gap of the material.

Recombination radiation was originally observed in natural diamond in 1960. Visible luminescence of diamond is mainly blue and ultraviolet emission from a strongly blue-luminescent diamond has been observed [84]. This led to the idea that LEDs could be made from diamond. Figure 1.13 illustrates the structure of a p-n junction diode made of diamond.

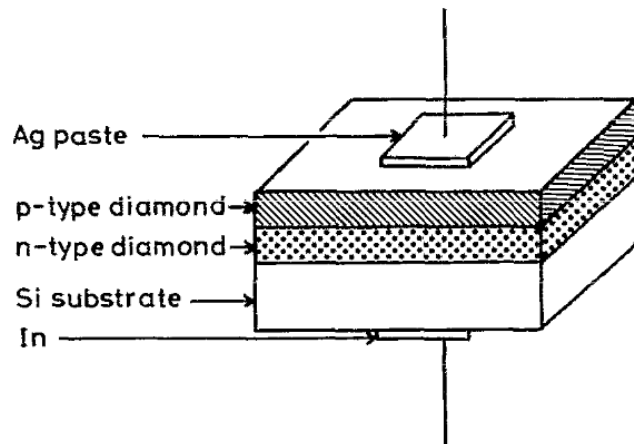


**Figure 1.13.** Structure a diamond p-n junction diode [85].

By suitable doping of diamond to produce a p-n junction, light emitting diodes have been made. A layer of boron-doped diamond was grown using trimethylboron and a layer of phosphorous-doped diamond was grown using phosphine. This produced the p-type and n-type diamond respectively. The result was main luminescent peaks from free exciton recombination at 235 nm and those from bound exciton recombination at 239 nm. The energies associated with the recombinations in this diamond are higher in energies than that of GaN (357 nm), an alternative LED material [86]. The depth profile for this p-n junction is given in Figure 1.14 and shows that the concentrations of the impurities is almost uniform through each layer and there is no intermixing at the p-n interface.

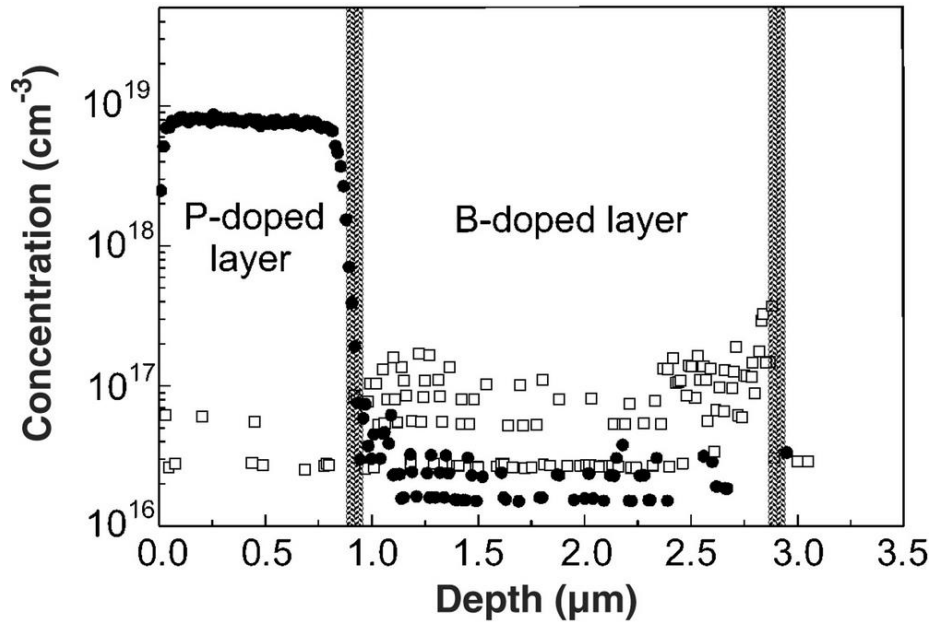


**Figure 1.14.** Impurity depth profile of a diamond p-n junction measured by SIMS, where solid circles represent phosphorus ( $^{31}\text{P}$ ) and open squares represent boron ( $^{11}\text{B}$ ) [86].

Diamond offers the advantage that its devices can operate at high temperatures and it is considered as a superior material for electronic applications [87]. By incorporation of nitrogen as an impurity to generate n-type diamond, a diamond p-n junction diode has been made which can demonstrate a diode characteristic at temperatures up to 900 °C; this is higher than any other material [88].

### 1.8.3 Thermionic Emission

Thermionic emission is the discharge of electrons from heated materials. It involves the displacement of an electron from the bulk of a material to the vacuum band – this is known as the work function and provides the barrier for thermionic emission.

A low electron affinity is a common property of thermionically emitting materials. Electron affinity is the energy required to remove an electron from a surface. Some materials, typically alkali-metal based materials, may even exhibit a negative electron affinity. In this case, the conduction band is raised above the vacuum band, as illustrated in Figure 1.15, and electrons are spontaneously emitted [89].

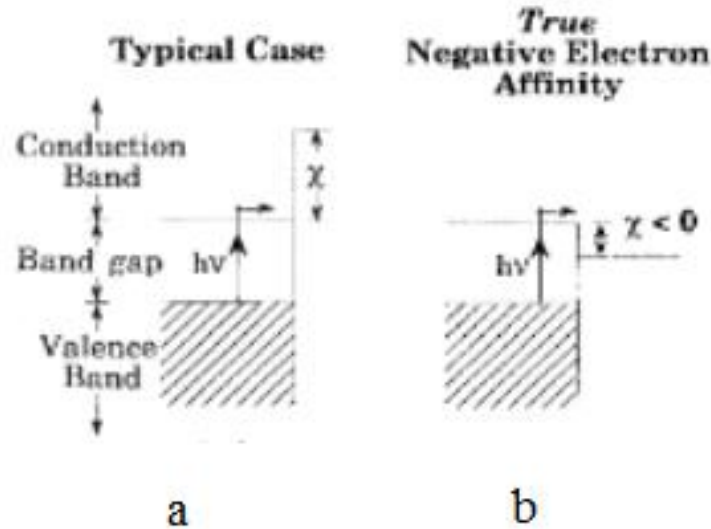


**Figure 1.15.** Electron affinity band diagrams showing a) positive electron affinity and b) true negative electron affinity [90].

The Richardson-Dushman equation gives the relationship between the emission current density,  $J$ , and the emitting material's work function  $\phi$  and  $A$  is an emission parameter [91]:

$$J = A_R T^2 e^{-\frac{\phi}{k_B T}}$$

Diamond is a suitable material for thermionic emission devices as shallow donor states and negative electron affinity would significantly lower the barrier for thermionic emission which could thus be observed at lower temperatures [91].

N-type diamond is more suitable for this effect than p-type diamond. Attempts have been made with phosphorus-doped diamond films which were found to demonstrate emission at temperatures less than 375 °C and the work function was 0.9 eV [91] which is lower than nitrogen-doped films which were also used [92]. Doping with lithium would also be expected to lower the work function [75].

The negative electron affinity of diamond can be obtained by controlling the termination of the film; hydrogen terminated diamond films show NEA whilst hydrogen-free surfaces do not [93]. Likewise lithium-oxide termination has been found to offer an NEA of - 3.9 eV [94].

Thermionic emitter devices have many uses including in fluorescent lamps, cathode ray tubes, X-ray tubes and thermionic converters [95]. Ultimately, solar heat could be concentrated, using lenses, onto a diamond film, resulting in the emission of electrons which could be used to create a circuit. In this way, solar energy could be turned into electricity; a renewable energy resource. This process is illustrated in the diagram below.

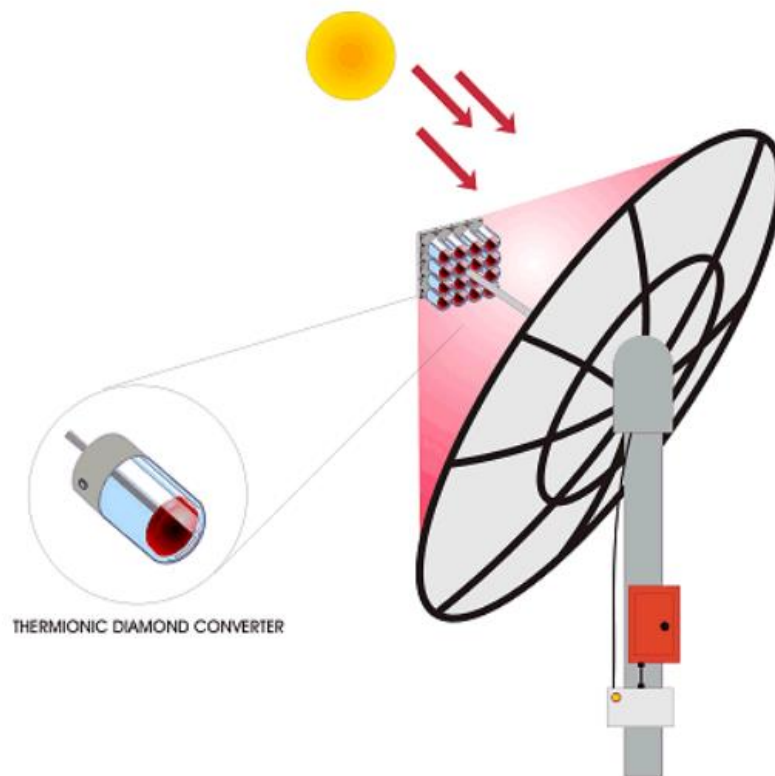


**Figure 1.16.** Diamond thermionic device [96].

## Chapter 2 Experimental Methods

### 2.1 Hot Filament reactor

Throughout this project, samples were prepared in a hot filament (HF) reactor system. For growing nitrogen-doped films and performing diffusions, a non-boron reactor was used. For growing boron-doped films a separate reactor was used as boron leads to contamination of the equipment.

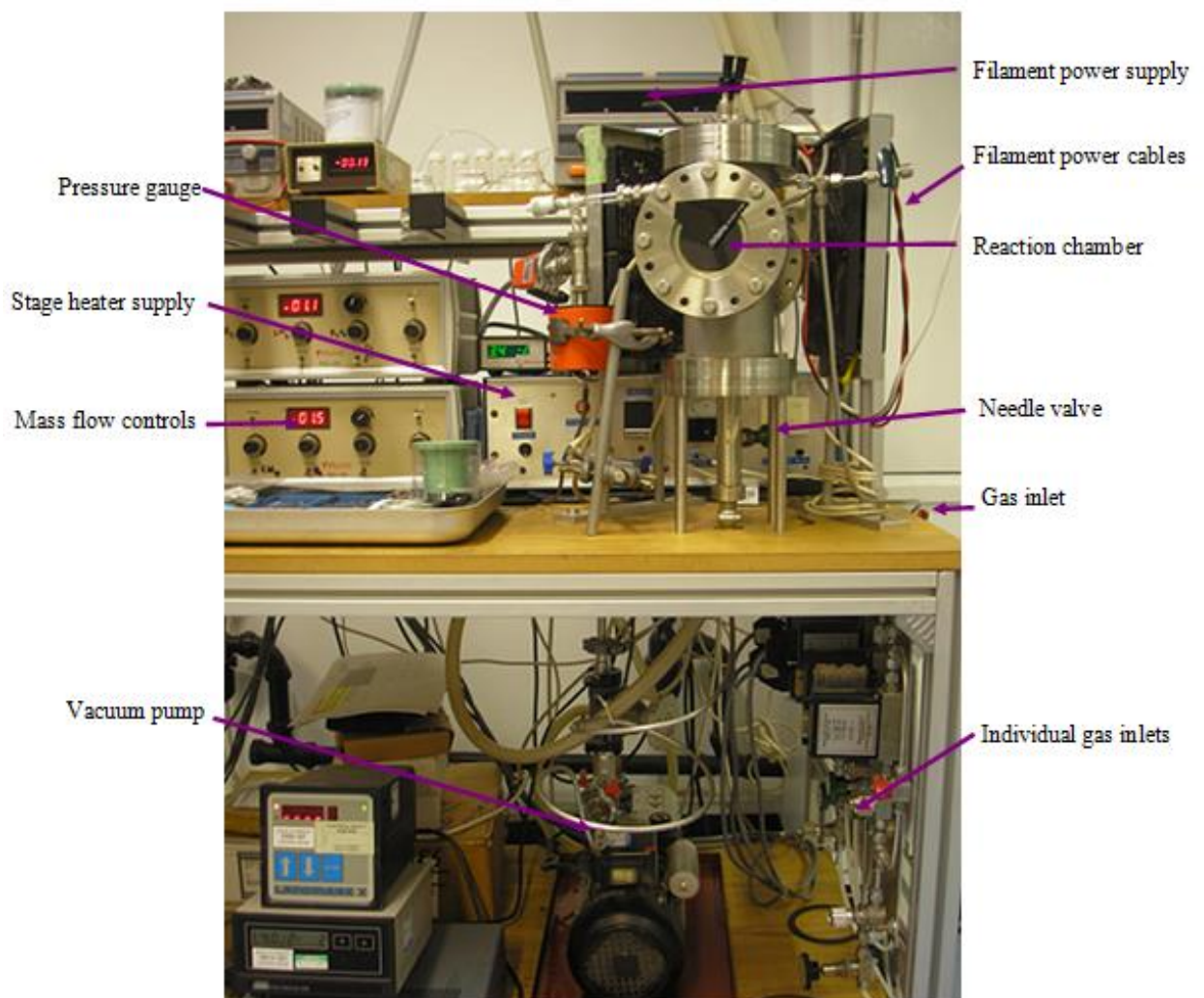


**Figure 2.1.** Non-boron hot filament reactor used in this study.

The non-boron and boron HF reactors contain filaments made of high melting point metals rhenium and tantalum, respectively. The filaments in both of reactors are suspended at 0.4 cm from the substrate holder.

The current applied across the filaments was maintained at 25 A throughout depositions and diffusions. The temperature of the filaments was approximately 2000 °C. The current applied to the substrate holder was 4 A and the temperature was approximately 600 °C. Overall, the temperature of the substrate was approximately 800 °C.

Before deposition the chamber was brought to vacuum pressure. The substrate heaters were preheated for 15 minutes in the non-boron reactor and 30 minutes in the boron reactor. After this time, the gases were added and the flow rates controlled by the mass flow controller (MFC). The chamber pressure was adjusted using the needle valve and was maintained at 20 Torr during the deposition.

The flow rates of methane and hydrogen were kept constant across the experiments and were 2.00 sccm for methane and 200 sccm for hydrogen (in order to grow microcrystalline diamond films).

The substrates used were n-type silicon (when doping with nitrogen) and p-type silicon (when doping with boron doping). All of the substrates were 1 cm<sup>2</sup>. The silicon substrates were prepared using a manual abrasion technique: alternating steps of scratching diamond powder into the substrate surface and cleaning with methanol.

## 2.2 Magnesium nitride suspension

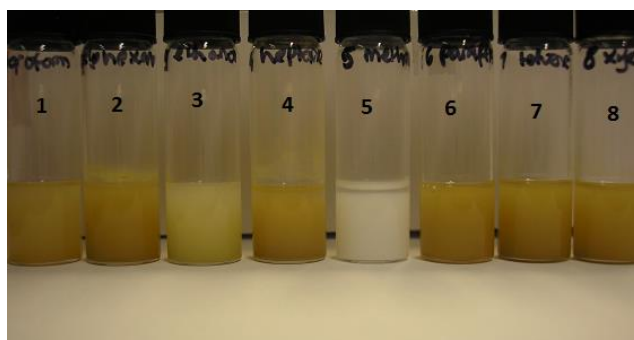
A study was carried out in order to find a stable suspension of Mg<sub>3</sub>N<sub>2</sub>. This would be required for the diffusion process and it would be necessary to have a suspension in which the particles were well-distributed and resistant to oxidation.

The solvents tested were chloroform, cyclohexane, ethanol, heptane, methanol, paraffin, toluene and xylene.

Suspensions were made using approximately 0.01 g of magnesium nitride, Mg<sub>2</sub>N<sub>3</sub> in 3 ml of solvent. These were placed in an ultrasonic bath for approximately 1 hour. The stability of the suspensions was monitored using an optical microscope, taking into account colour (to the eye as well as under an optical microscope), physical appearance, particle distribution in the solvent

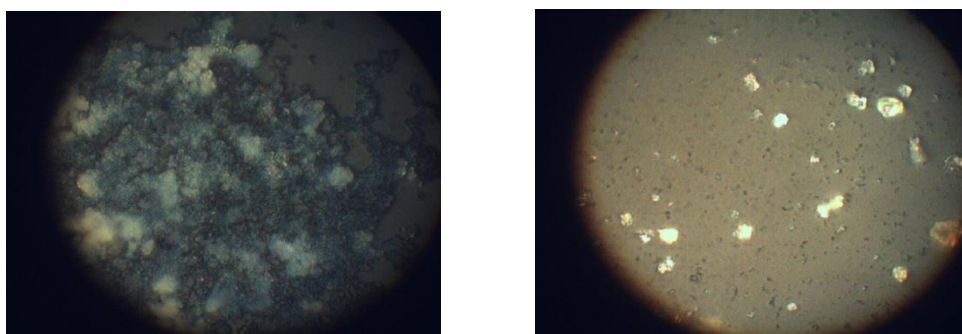
(noting any clumping), particle size and how long the suspensions remained suspended after sonication.

The suspensions initially had a cloudy yellow appearance (Figure 2.2). However, it is clear that suspensions made with ethanol, 3 and methanol, 5 are less stable than the other solvents. The yellow appearance is faded with ethanol and in the case of methanol, the suspension is white. The suspension in methanol formed this white colour quickly - as early as day 1 (suspensions made on day 0).



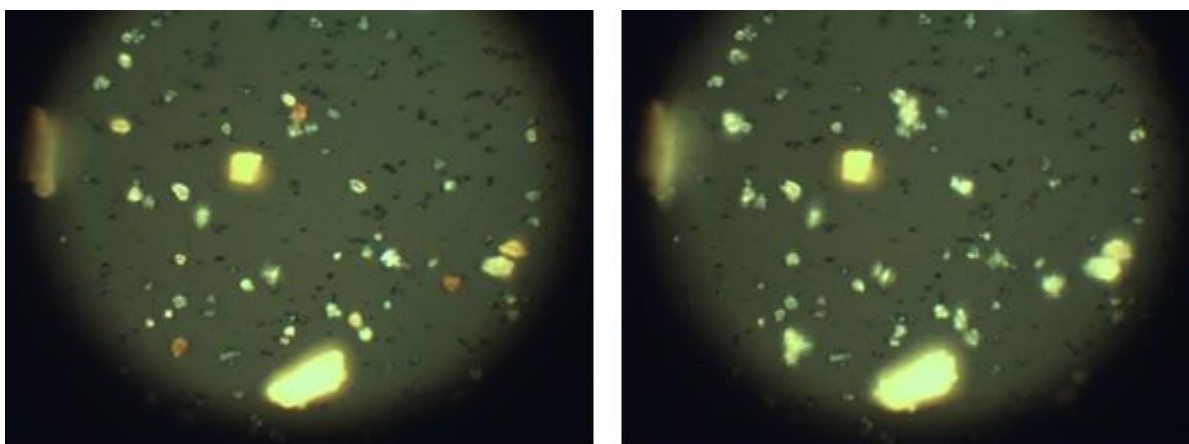
**Figure 2.2.** Suspensions on day 3.

Figure 2.3 shows the magnified methanol and ethanol suspensions on day 3. The methanol has interacted undesirably with the compound and the image of the suspension formed in ethanol shows the particles are white, indicating oxidation of the  $Mg_3N_2$ .



**Figure 2.3.** Left: suspension in methanol  $\times 1000$  day 3, right: suspension in ethanol  $\times 1000$  day 3.

Polymers (polysorbate and Brij78) were also investigated to improve particle distribution and resistance to oxidation. On exposure to air, the suspensions without polymer suffered fading in colour after a couple of minutes as shown in Figure 2.4, with xylene as an example.



**Figure 2.4.** Xylene suspension left: immediately after deposition, right: a few minutes after deposition.

Paraffin, toluene and xylene were deemed unsuitable solvents as their suspensions took too long to dry to be of practical use.

The most successful suspension seemed to be chloroform with polysorbate: the solid was well distributed throughout the suspension and the suspension was resistant to oxidation. There was little clumping together of the particles. The colour of the suspension, to the eye, kept its yellow colour for at least two weeks. Using the optical microscope, the particles were also seen to retain their colour over this period.

### 2.3 The diffusion process

In order to diffuse the magnesium into the diamond films, a film (either nitrogen-doped or boron-doped) was grown for 4 hours, the sample was then removed from the reactor and the magnesium nitride suspension was dropcast on top of the diamond film and allowed to dry. This was done using a micropipette and in 50  $\mu\text{l}$  amounts (maximum amount held on substrate). The sample was then returned to the reactor and the process was repeated as before. However, for 1 hour, only hydrogen gas entered the chamber. After one hour, methane was added in order to grow a thin capping layer of diamond on top. This method follows that of the lithium/nitrogen co-doping method, presented in [68]. Figure 2.5 shows the general structure of the sample made in this study with the orange region indicating the area in which magnesium will be expected to be found following diffusion.

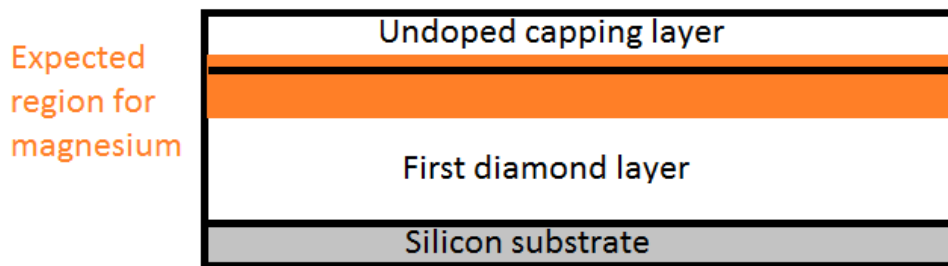


**Figure 2.5.** General structure of films grown in this study (not to scale).

## 2.4 Scanning electron microscopy

Scanning electron microscopy (SEM) was used to analyse the surfaces of the films produced. There are a number of advantages of using this type of microscopy instead of optical microscopy: SEM has a large depth of field which means that a large amount of the sample can be in focus at one time; it is also possible to obtain high quality images at higher magnification (up to  $\times 100\,000$ ) as SEM has a high resolution [97].

SEM is an *ex-situ* technique [98] in which primary electrons are aimed at the sample and cause the release of secondary electrons (Figure 2.6) which are detected and send an electrical signal to a video screen to produce the image which has a resolution of approximately 50 nm [99].

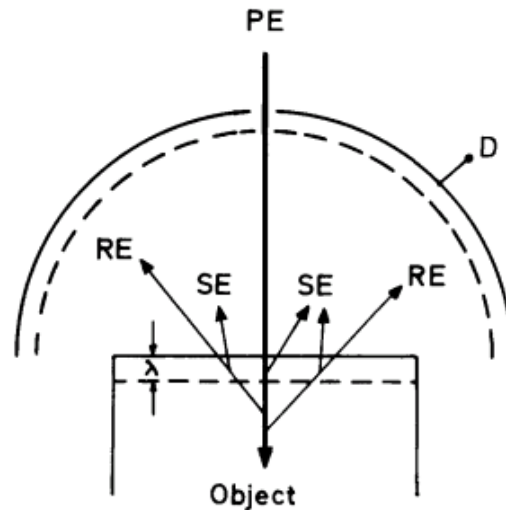


**Figure 2.6.** SEM mechanism: Secondary electrons (SE) are released by primary electrons (PE) and by backscattered or reflected electrons (RE) [100].

It is used to provide images of diamond films which can be used to obtain information such as film thickness and film morphology. Using SEM, the morphology of the films grown in these experiments was investigated.

## 2.5 Secondary ion mass spectrometry

Secondary ion mass spectrometry (SIMS) was used to analyse the composition of the films. It is a technique commonly used for analysing the charge carriers in semiconductors [101]. Indeed it can be used to analyse the composition of diamond films [102] and may be used to monitor the behaviour of impurities or dopants through a diamond film to produce a depth profile as seen in Figure 2.7. This has been important for characterising thin films used in microelectronics and materials science [103].

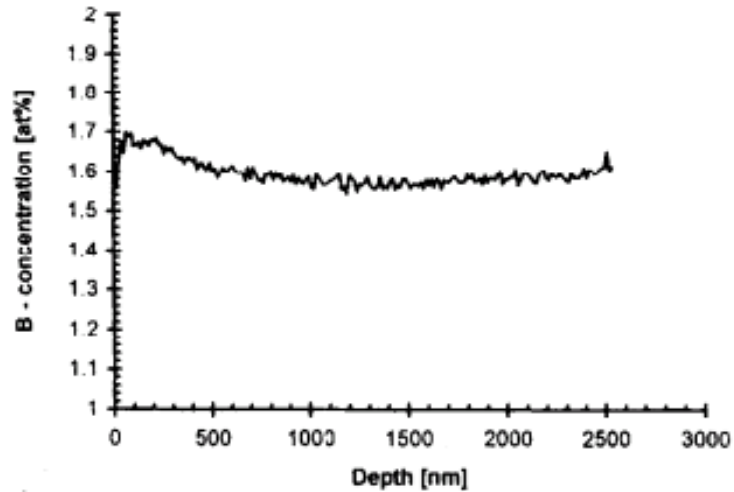


**Figure 2.7.** SIMS depth profile of B through a diamond film [102].

The process of SIMS involves a high energy primary beam of 250 eV – 30 keV (in this study a gallium beam was used) which bombards a surface [104] and starts a cascade of collisions between the impacting particle and the atomic nuclei in the sample, resulting in the emission of atoms or clusters which are ionized and monitored [101]. There are two types of SIMS: static, which analyses the surface, and dynamic, which generates a depth profile of the substance [105].

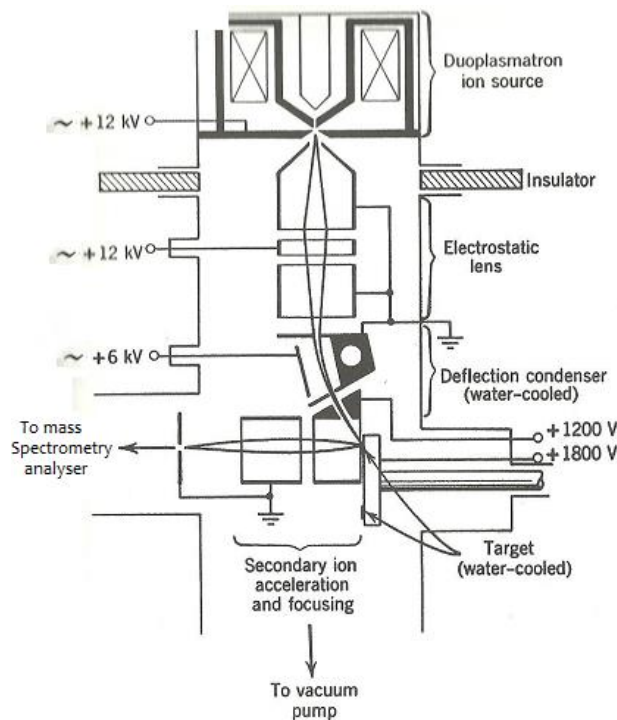


**Figure 2.8.** A schematic diagram of the SIMS setup [106].

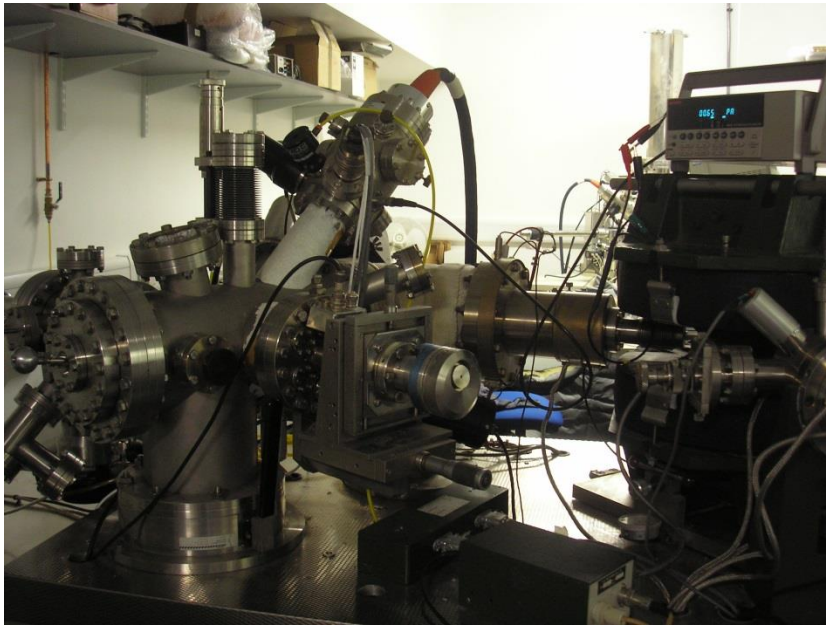


**Figure 2.9.** SIMS setup used in this study.

The data is obtained as ion counts versus time. Using a calibration sample, this is converted to density (or concentration) versus depth, to give a depth profile. The conversion to density is made using an ion implanted standard – a sample implanted with a known amount of impurity (this is done for each separate ion that is detected).

The conversion to depth is made by calculating the etch rate which can be found by measuring the sputter crater depth after the analysis is completed and is done accurately by using a calibration sample [107].

In this study, nitrogen concentration was calculated in SIMS as there is a suitable calibration sample. The intensity of the  $CN^-$  ion (used to measure N) is given as a ratio to the  $C^-$  ion (constant throughout the film) to remove the effect of any slight fluctuation in intensity. The ratio is then converted to concentration.

## 2.6 Energy-dispersive X-ray spectroscopy

Energy-dispersive X-ray spectroscopy was used to determine the elemental composition of the diamond films. The process is used with SEM and involves the analysis of X-rays emitted from the atoms composing the film. Characteristic X-rays are emitted from the solid surface when it is struck by a beam of high energy electrons [108]. In the case of EDX, these X-rays are measured by their energy which allows the elements composing the specimen under examination to be determined [109].

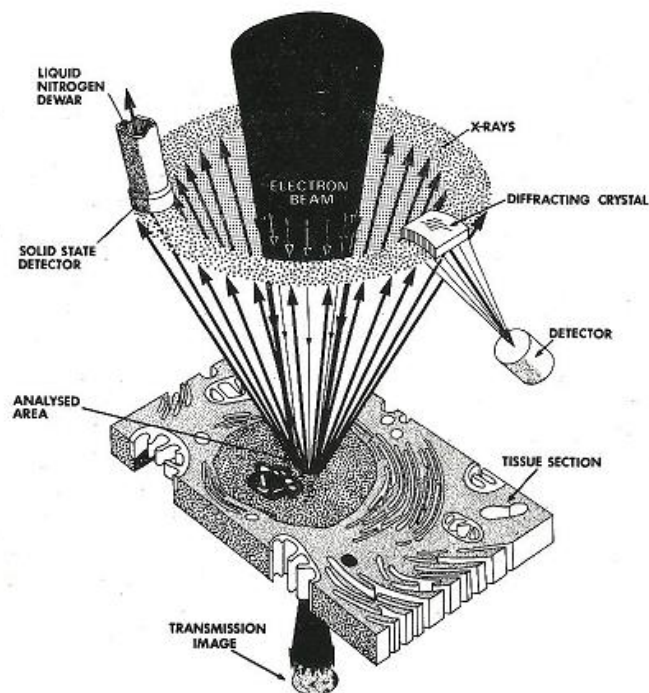


**Figure 2.10.** A schematic diagram of the X-Ray analysis from an ultrathin specimen [110].

## 2.7 Conductivity measurements

Conductivity of the films was measured using a simple 2-point probe. First, 2 small dots were placed on the samples at a distance of 0.4 cm using conductive silver paint, shown below (Figure 2.11).

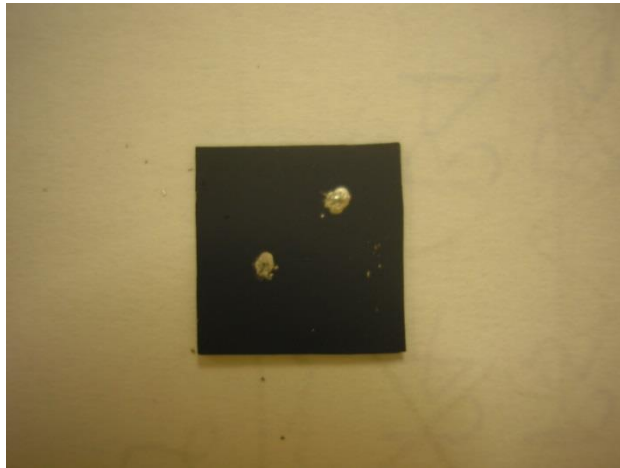


**Figure 2.11.** Sample prepared for resistivity measurements.

The samples were next ozone treated in a UV/ozone treatment machine for 30 minutes. This removes hydrogen termination of the films and ensures oxygen termination. Hydrogen termination affects the surface conductivity; the bulk conductivity was to be measured so surface conductivity needed to be eliminated. Multiple measurements of the resistivity were taken on each sample and averages were calculated.

## Chapter 3 Results and Discussion

### 3.1 Scanning Electron Microscopy (SEM)

SEM was used to analyse the morphology of the films grown in this study and determine the effect of different growing conditions upon the morphology.

When producing nitrogen-doped diamond films, the flow rate of ammonia is known to have an impact on the film morphology [111]. This can be seen in Figure 3.1 where a lower flow rate of ammonia of 0.2 sccm produced well-defined (100) square facets, which are approximately 1 $\mu$ m in size. Whereas, a higher flow rate of 0.75 sccm, creates larger facets. Although 0.75 sccm also produces square facets, the size of the facets is smaller, less than 1 $\mu$ m and some of the facets are less well defined. At 1 sccm, the film is no longer uniform.

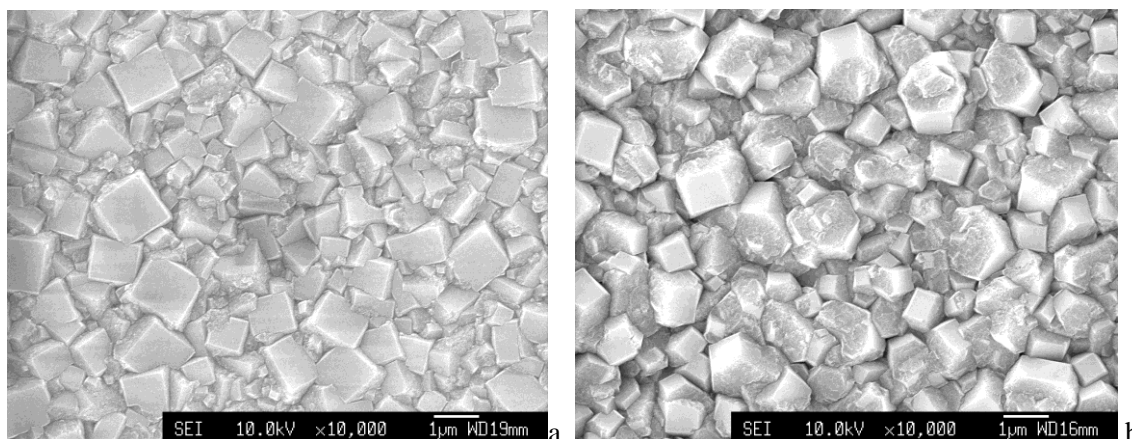


**Figure 3.1.** SEM images of nitrogen-doped diamond films at ammonia flow rate a) 0.2 sccm and b) 0.75 sccm. Grown on n-type silicon.

When diffusing magnesium into nitrogen-doped films, it was found that the ammonia flow rate affected the incorporation of magnesium. Attempts to diffuse magnesium into films grown with 0.75 sccm ammonia resulted in a deposit (of  $Mg_3N_2$ ) remaining on top of the sample after diffusion and subsequent growth of the capping layer (Figure 3.2). This was not the case with 0.2 sccm of ammonia which appeared to produce a clean, smooth surface where all the  $Mg_3N_2$  had diffused into the film after the same diffusion and capping procedure. This suggests that the 0.75 sccm flow rate is too high whilst the 0.2 sccm flow rate permits magnesium incorporation. No other flow rates were used as these do not form the (100) square facets that are desired. Diamond has a very tight lattice which makes it extremely difficult for other atoms to fit. At a higher flow rate of ammonia, more nitrogen will be incorporated into the diamond, leaving less space for any

magnesium. A comparison of the amount of nitrogen incorporated when diffusing different amounts of  $Mg_3N_2$  could be made using SIMS.

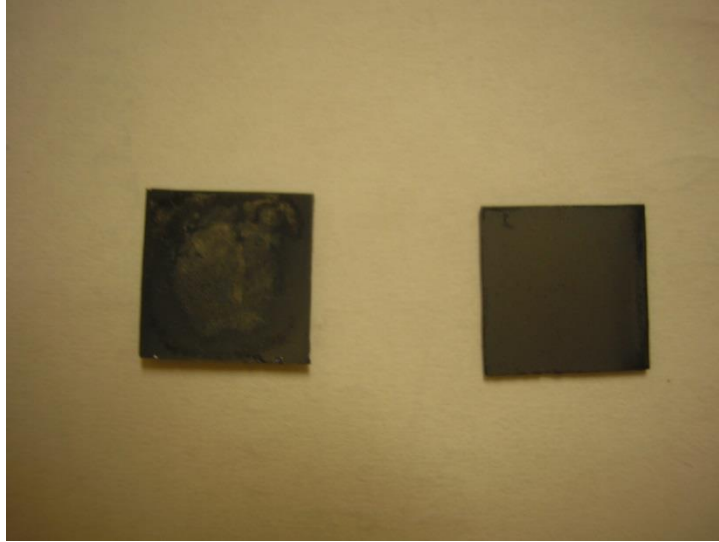


**Figure 3.2.** Photographs of nitrogen-doped diamond films. Left: ammonia flow rate 0.75 sccm, right: ammonia flow rate 0.2 sccm. Magnesium diffusion was carried out on both films.

When magnesium has been diffused into nitrogen-doped diamond films, square facets appear as expected, however these are ‘roughened’, as shown in Figure 3.3, compared to those with no magnesium. This suggests that the magnesium may etch the surface, creating new nucleation sites. A similar observation was made when lithium was diffused into a nitrogen-doped film [68].

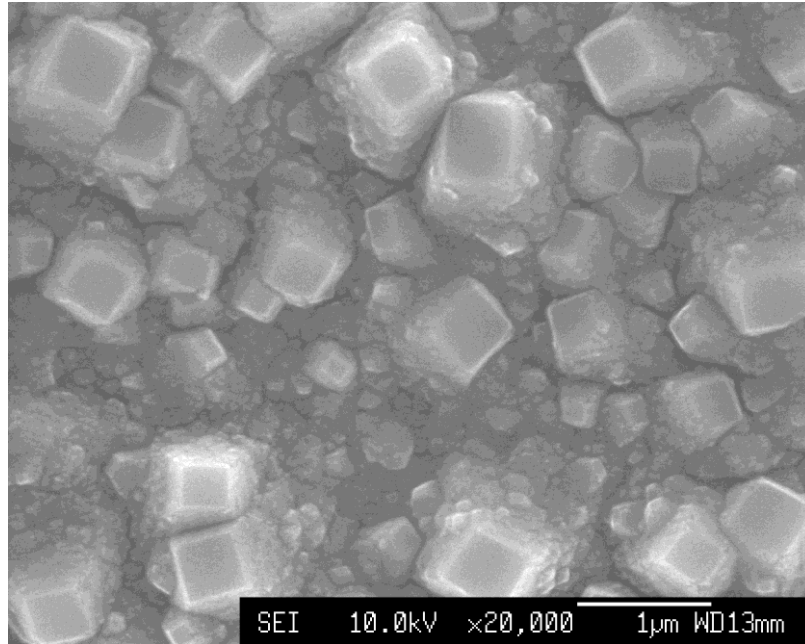


**Figure 3.3.** SEM image of magnesium diffused into nitrogen-doped diamond film (ammonia flow rate 0.2 sccm). Grown on n-type silicon.

Diffusing magnesium into a boron-doped film created twinned facets as expected, shown in Figure 3.4. The facets are on the microcrystalline scale and as the boron concentration is increased the triangular  $\{111\}$  facets predominate over the  $\{100\}$  facets, as shown in previous studies [112]. Unlike the nitrogen-doped films, the higher diborane flow rate 0.5 sccm was suitable for incorporating magnesium; no deposit remained on the surface after diffusion. Compared with the boron films not diffused with magnesium, these are slightly ‘roughened’ although not as big a difference is seen as with the nitrogen-doped samples.

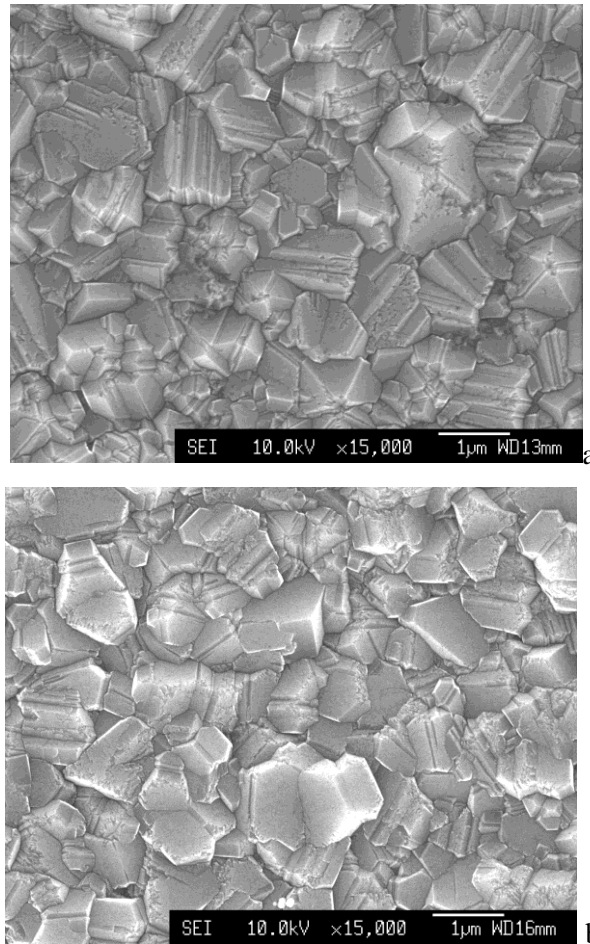


**Figure 3.4.** SEM images of magnesium diffused into boron-doped diamond films (diborane flow rate a) 0.1 sccm b) 0.5 sccm). Grown on p-type silicon.

### 3. 2 Secondary Ion Mass Spectrometry (SIMS)

SIMS was used in order to identify the composition of the diamond films. By monitoring the intensity of various ions, it was possible to predict the composition and indicate whether magnesium had been incorporated into the diamond film. In positive SIMS, the positive ions of C, Mg and MgO were detected. In negative SIMS, the negative ions of C, CN and C<sub>2</sub> were detected.

However, this method detects ions according to their mass and as the mass of the magnesium ion matches the mass of the C<sub>2</sub> ion, the intensity measured cannot be assigned exclusively to C<sub>2</sub> or Mg. It is noted that C<sub>2</sub> is indeed an extremely probable ion to be emitted from the diamond surface. Experiment 1 (below) was designed to overcome this problem. Alternatively, the magnesium oxide ion could be measured. Magnesium oxide may form as a secondary ion emitted from the sample if oxygen is present in the film so detecting this ion would be an indication of

any magnesium incorporated into the film. As magnesium oxide and calcium, which could easily contaminate the sample, have the mass 40, the same problem occurred again. Experiment 2 was designed to overcome this problem.

## Experiment 1

A nitrogen-doped layer was first grown for 4 hours, the magnesium suspension was then deposited and diffused in a hydrogen atmosphere for 1 hour and finally another nitrogen-doped layer (same conditions as the first layer) was grown for a further 3 hours. As illustrated in Figure 2.5, the region between the layers contains the magnesium which is expected to diffuse slightly into the first and the top layer of the diamond.

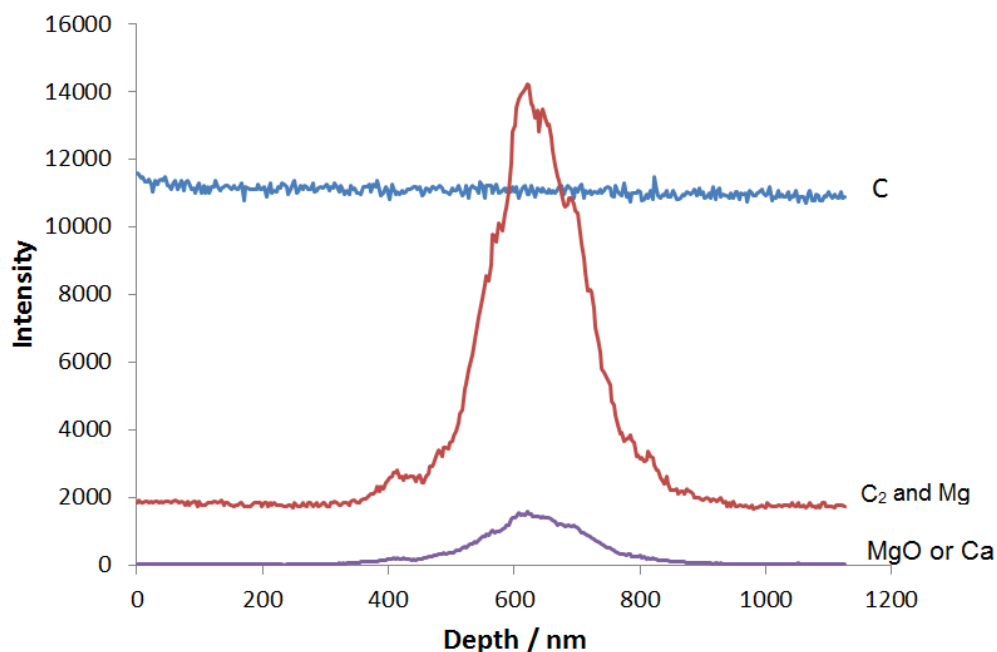
Figure 3.5 shows the information obtained from positive SIMS, in which the intensity of the carbon ion was measured, along with the ions of mass 28 which will be both  $C_2$  and Mg, as well as the ions of mass 40 which may be MgO or Ca.

The  $C_2$  and Mg signal peaks at around 650 nm. Either side of this peak, in the regions of depth less than 400 nm and greater than 800 nm, the base line intensity of the  $C_2$  ion can be seen. This shows the area of the film where no magnesium was expected and the film composition was constant. There is no reason for the amount of  $C_2$  ions to increase at any point through the depth profile, suggesting that the increase in the mass 24 signal is due to the presence of magnesium ions which have been incorporated into the diamond film. The depth of 650 nm is therefore where the magnesium was added and allowed to diffuse. The broadening of the peak, of approximately 200 nm in both directions, is likely due to the diffusion of magnesium – down into the first diamond layer and up into the layer grown on top. However, this could be influenced by SIMS mixing, a machine dependent factor where the different roughness of different surfaces may influence the sharpness of any layer boundaries. In order to confirm if this was a factor, further tests would need to be done: SIMS could be performed on films of approximately the same thickness but with different morphologies (therefore, different surface roughness) and the results (in particular, the peak broadening) could be compared. It would thus be possible to see if the peak broadening was affected by the surface roughness [68].

It can be seen that the carbon intensity remained constant throughout the film as expected. This is because the first layer (grown for 4 hours) and the second layer (grown for 3 hours) are grown under the same conditions.

Figure 3.5 also shows a peak for the mass corresponding to the MgO or Ca ion, this is in the same position as the Mg peak. It could be due to an increase in magnesium oxide being emitted as a

secondary ion at this point. Alternatively, it may be owing to an increase in calcium. This would be possible as calcium may contaminate the sample when it is removed from the reactor to deposit the magnesium. In order to obtain a more conclusive result, a further experiment (experiment 2) was carried out.



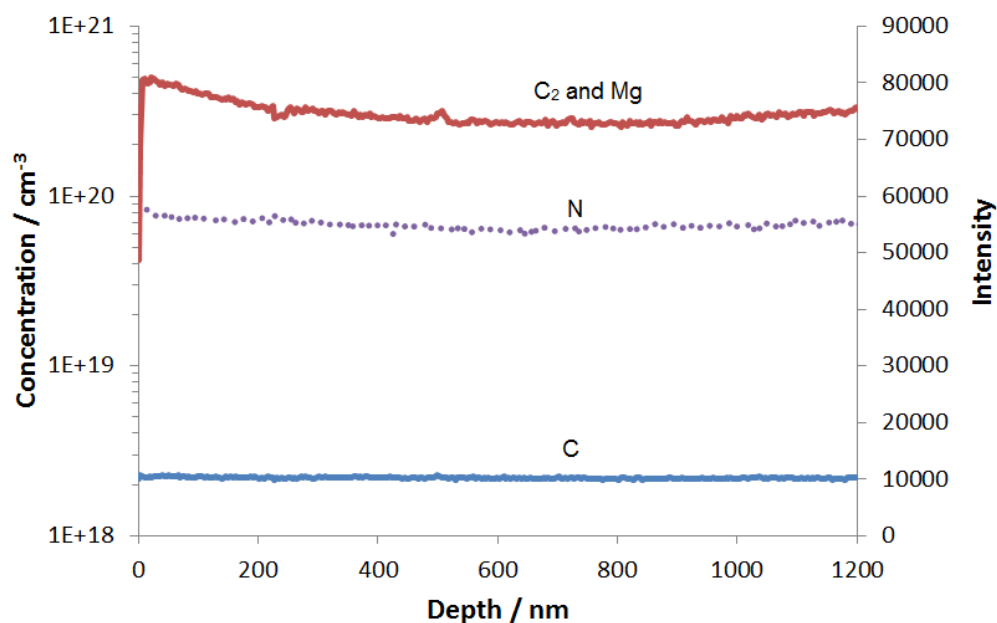
**Figure 3.5.** Depth profile of sample grown under 0.2 sccm  $\text{NH}_3$  and with 100  $\mu\text{l}$  of  $\text{Mg}_3\text{N}_2$  solution diffused into it. SIMS performed with positive mode, electronic gating on, magnification of  $\times 5000$  and ion beam current at 3 nA.

Figure 3.6 shows the negative SIMS method which measured the intensity of secondary ions with mass 12 ( $\text{C}^-$  ion), 24 (which could be either  $\text{C}_2^-$  or  $\text{Mg}^+$  ion) and 26 ( $\text{CN}^-$  which allows us to track the nitrogen content of the film). The nitrogen ion was measured as  $\text{CN}^-$  ion and a concentration was obtained using a calibration sample which was implanted with a known amount of nitrogen.

All the signals in this spectrum are constant with depth, as expected. As magnesium is unlikely to form a large quantity of negative ions, the ions of mass 24 can be assumed to be all  $\text{C}_2^-$ , which will be constant throughout the film. Likewise, the intensity of C ions measured will be constant throughout the film. The nitrogen-doping was produced by using ammonia as a precursor gas and the flow rate of which was kept constant throughout growth and was the same for both the first and second layers. As such, a constant measure of the nitrogen concentration is seen throughout the depth profile.

These results are similar to those obtained in similar experiments with lithium. The SIMS spectrum, presented in Figure 1.11 shows that the lithium also diffuses in the diamond, indicated

by a broadened peak. In the case of lithium, the diffusion was also approximately  $\pm 200$  nm [68]. This is consistent with the  $\text{Mg}^{2+}$  ion being smaller than the  $\text{Li}^+$ , allowing it to diffuse more readily through the film. There is also a slight asymmetric character to the  $\text{C}_2/\text{Mg}$  peak in Figure 3.5, as with lithium, but this may be due to the additional time magnesium has to diffuse down into the film compared to upwards into the film grown on top after the initial diffusion period.



**Figure 3.6.** Depth profile of sample grown under 0.2 sccm  $\text{NH}_3$  and with 100  $\mu\text{l}$  of  $\text{Mg}_3\text{N}_2$  solution diffused into it. SIMS performed with negative mode, electronic gating on, magnification of  $\times 5000$  and ion beam current at 3 nA.

## Experiment 2

In order to determine the origin of increase of the intensity of the ion with mass 40 (magnesium oxide or calcium), illustrated in Figure 3.5, a second experiment was carried out. In this experiment a sample was prepared under the same conditions as before except no magnesium-doping occurred: a nitrogen-doped diamond layer was first grown for 4 hours and then a second nitrogen-doped diamond layer was grown. However, after the first layer was grown, the sample was removed from the reactor for 10-15 mins, as if the diffusion were to be carried out, but no magnesium was added. This was done in order to determine if any calcium contamination occurred.

Figure 3.7 shows the positive SIMS spectrum from experiment 2. Here, there is no peak in the signal monitoring ions of mass 40. If calcium contamination were to occur with removal of the

sample, an increase in the signal would be expected. However, as there is no increase in the intensity, this implies that there is no calcium contamination and the peak in Figure 3.5 is likely to be caused by emission of secondary magnesium oxide ions (although magnesium is not necessarily bonded to oxygen within the bulk of the diamond).

The intensity and concentrations of the other species remain approximately constant as expected: the C ion will be constant in concentration throughout the film and the C<sub>2</sub>/Mg signal will be entirely due to C<sub>2</sub> ions (as no Mg-doping was carried out in this experiment) and this intensity should remain constant throughout the film.

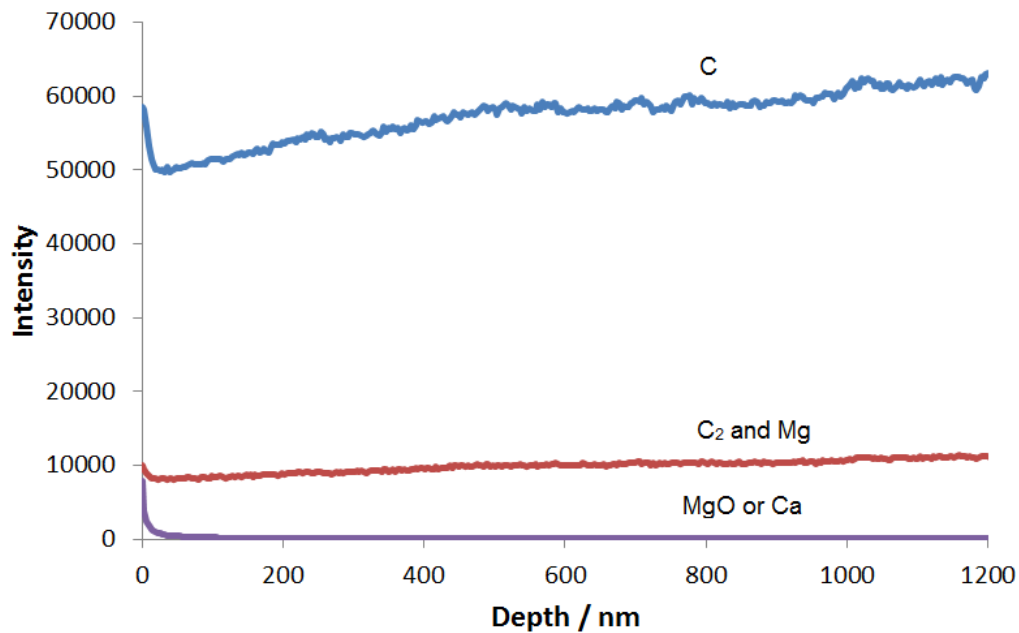


**Figure 3.7.** Depth profile of sample grown under 0.2 sccm NH<sub>3</sub> and with no Mg<sub>3</sub>N<sub>2</sub> solution diffused into it. SIMS performed with positive mode, electronic gating on, magnification of × 5000 and ion beam current at 3 nA.

Figure 3.8 shows the negative SIMS spectrum of the second experiment. As expected the intensity of the negative ions remains constant throughout the depth profile for the same reasons discussed above.

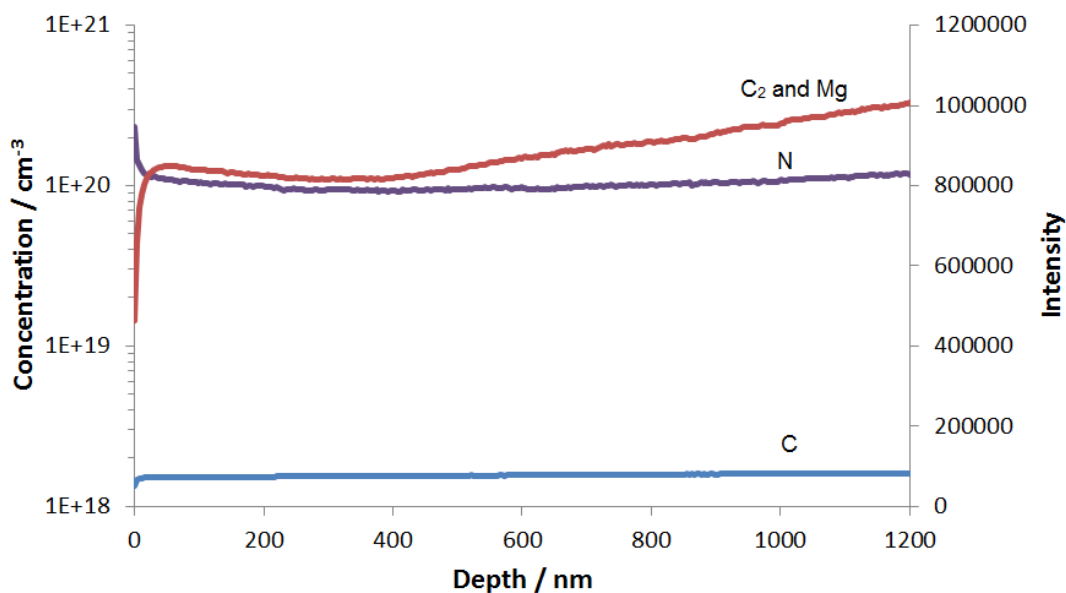


**Figure 3.8.** Depth profile of sample grown under 0.2 sccm  $\text{NH}_3$  and with no  $\text{Mg}_3\text{N}_2$  solution diffused into it. SIMS performed with negative mode, electronic gating on, magnification of  $\times 5000$  and ion beam current at 3 nA.

With a calibration sample, it will be possible in future experiments to determine the concentration of magnesium present in the films as outlined in Experimental Methods. The SIMS results of a calibration sample (implanted with a known amount of magnesium) would also need to be compared to a sample grown under the same conditions but with no magnesium diffused into it to verify that the baseline  $\text{C}_2$  was of the same intensity in each.

### 3.3 Energy-Dispersive X-Ray Spectroscopy (EDX)

EDX was another method used to identify the elemental composition of the diamond films. It was used as an indication of whether magnesium was present in the films.

Samples were analysed where magnesium had been diffused into nitrogen-doped diamond films. Although, there seem to be peaks at the correct energy for magnesium, these are not easily distinguished from the shoulder of the silicon peak. By reducing the acceleration voltage, the electron beam will penetrate less into the film, resulting in less detection of silicon from the underlying substrate. However, as the magnesium has a weak signal, the acceleration needs to be sufficient to generate a count that is high enough to be sure it is not just noise. As these films are relatively thin, silicon was detected even with a slight reduction in the acceleration voltage. By

taking measurements at different points on the surface and by varying the magnification, the peaks were sometimes more defined as shown in Figure 3.9 b but not enough to be certain of their nature.

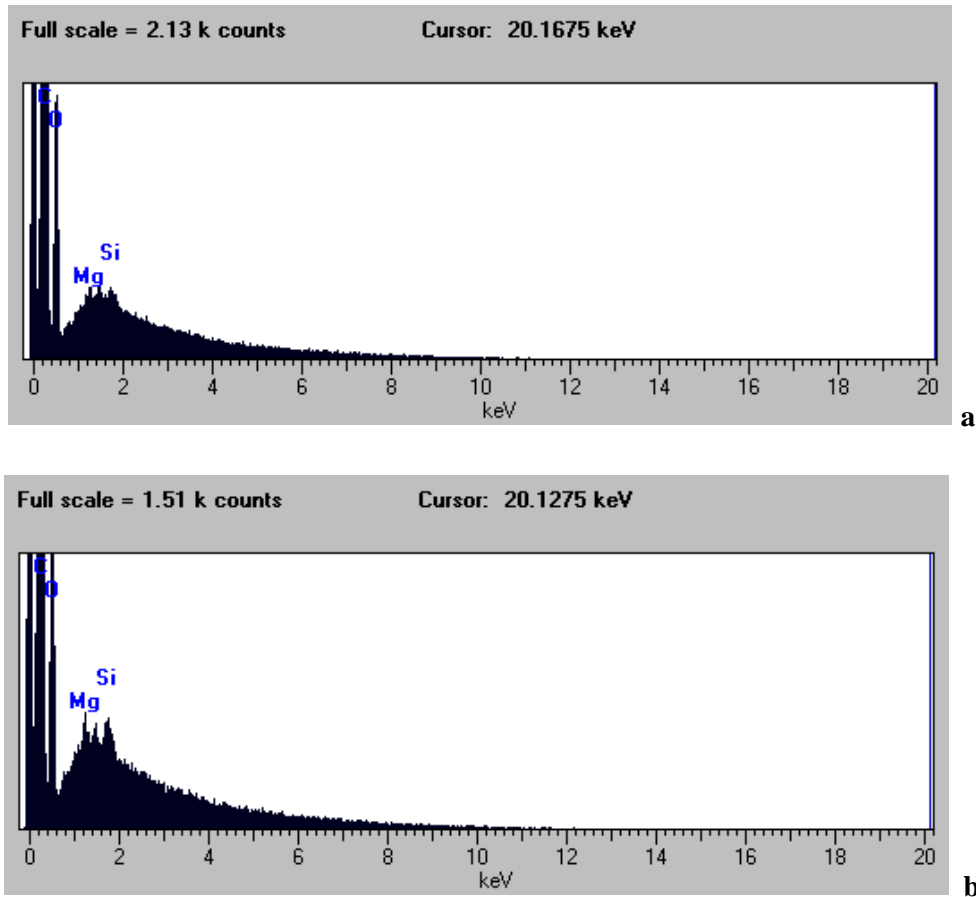


**Figure 3.9.** EDX spectra of films of magnesium diffused into nitrogen-doped diamond (ammonia flow rate: 0.2 sccm). EDX carried out at magnification a)  $\times 1000$  and b)  $\times 200$ , acceleration voltage 13kV and spot size 40. Sepctra a and b correspond to different points on the surface.

When analysing samples where magnesium had been diffused into boron-doped diamond films, the magnesium peak is more pronounced and easier to distinguish from the silicon peak, shown in Figure 3.10 and Figure 3.11. This may be explained by the boron-doped films being slightly thicker than the nitrogen-doped films. Indeed, a high level of ammonia in the gas mixture is found to slow the growth rate of diamond [111]. The thicker boron-doped films would mean there would be a reduced silicon signal with the same acceleration voltage compared to the nitrogen-doped films.

EDX was performed on two samples which were grown under the same conditions, varying only in the amount of  $Mg_3N_2$  solution that was diffused into them. The first sample was produced by 100  $\mu l$  amounts of  $Mg_3N_2$  solution being diffused into the film and for the second sample, 150  $\mu l$  of  $Mg_3N_2$  were diffused. The second sample would be expected to contain more magnesium and the ratio of B:Mg peaks to be different. By taking a ratio of the size of the magnesium peak to the boron peak for the different samples, the relative amounts of magnesium incorporated into the different samples can be found. Only, the relative amounts can be considered as EDX has a different sensitivity for different elements and requires a sensitivity factor in order to convert counts into concentration.

The ratios were taken for the spectra below and the average was calculated. It was found that the second sample made with a larger amount of magnesium nitride solution had a smaller average Mg:B peak ratio of 0.027 compared to 0.049. This implies that there was more magnesium in the film compared to the first sample, as expected since a larger volume of magnesium was deposited.

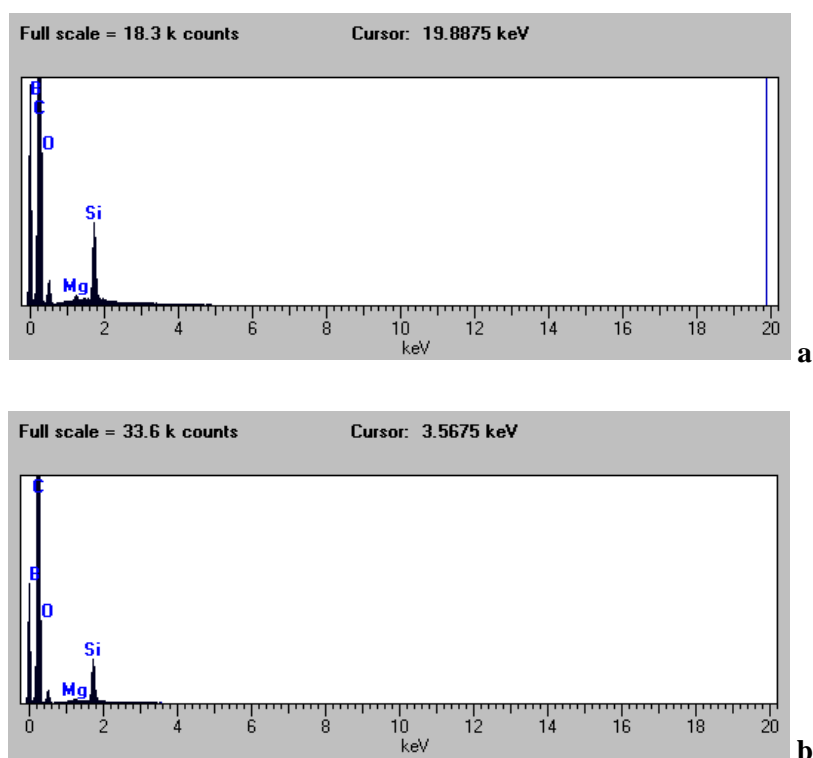


**Figure 3.10.** EDX spectra of films of magnesium diffused (total of 100  $\mu l$ ) into boron-doped diamond (diborane flow rate: 0.1 sccm). EDX carried out at magnification  $\times 200$ , acceleration voltage 13 kV and spot size 40. Spectra a and b correspond to different points on the surface.

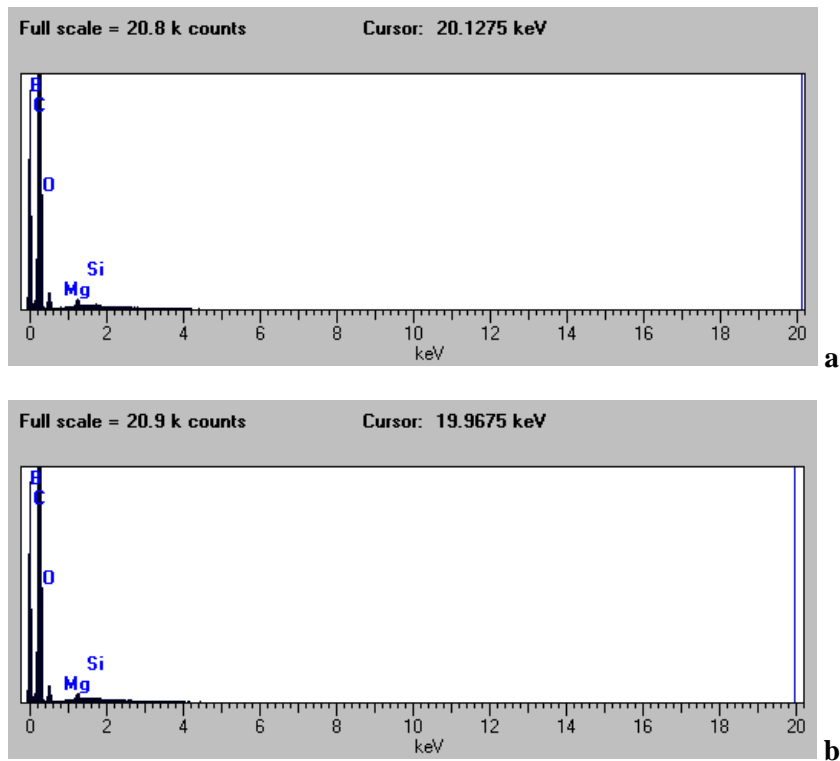


**Figure 3.11.** EDX spectra of films of magnesium diffused (total of 150  $\mu\text{l}$ ) into boron-doped diamond (diborane flow rate: 0.1 sccm). EDX carried out at magnification a)  $\times 200$  and b)  $\times 950$ , acceleration voltage 13 kV and spot size 40. Spectra a and b are taken at different points on the surface.

This method can provide some indication of whether magnesium is in the films and has thus been incorporated and in some cases provides an indication of the relative amount of magnesium present. Despite this, the information is not accurate as certain elements have signals which are close in proximity and can overlap. In addition, it is not possible to determine how magnesium exists in the film from these results; it is unclear whether magnesium is residing on substitutional or interstitial sites or whether it is located in the grain boundaries of the microcrystalline film. Also, this technique is qualitative and not quantitative and so samples can only be compared.

### 3.4 Conductivity Measurements

Conductivity of the films was measured using the 2-point probe method. Conductivity is important in order to determine the material's suitability for electronic applications which require a low resistivity. Additionally, a low resistivity will improve the efficiency of thermionic emission. A boron-doped film will not emit but by incorporating magnesium the emission

properties are expected to change. In doing so, the conductivity of the film may be deteriorated – the extent of which was investigated.

### Experiment 3

Sample	Average resistivity	Uncertainty ( $\pm$ )
Nitrogen-doped + low magnesium concentration	>20 M $\Omega$	N/A
Nitrogen-doped + high magnesium concentration	>20 M $\Omega$	N/A
Boron-doped + low magnesium concentration	1927 $\Omega$	16.5
Boron-doped + high magnesium concentration	1355 $\Omega$	37

**Table 3.1.** Resistivity measurements taken in experiment 1.

Magnesium was diffused into both nitrogen-doped diamond films and boron-doped films. A high and a low magnesium concentration were both tested. The resistivity of the nitrogen-doped films diffused with magnesium was high, as expected, and too high to measure with this method, >20 M $\Omega$ . However, magnesium diffused into boron-doped films created a film with lower resistivity that could be measured. It was found that varying the magnesium concentration affected the conductivity - higher magnesium concentration leading to higher conductivity. This suggests that the magnesium is influencing the electronic properties of the diamond films.

### Experiment 4

Sample	Diborane flow rate (sccm)	Mg <sub>3</sub> N <sub>2</sub>	Average resistivity	Uncertainty ( $\pm$ )
A	0.5	None	12.7 $\Omega$	3.4
B	0.5	Low concentration	881.6 $\Omega$	6.5
C	0.5	High concentration	313.6 $\Omega$	0.5

**Table 3.2.** Resistivity measurements taken in experiment 2.

In order to confirm the effect of the magnesium, a series of three boron-doped diamond films were grown, each under the same conditions (0.5 sccm diborane film grown for 4 hours, Mg<sub>3</sub>N<sub>2</sub> deposited and diffused for 1 hour in hydrogen atmosphere, and capping layer grown for 15

minutes). Sample A had no  $Mg_3N_2$  solution diffused into it, sample B had 100  $\mu l$  of low concentration  $Mg_3N_2$  solution diffused into it, and sample C had 100  $\mu l$  of high concentration  $Mg_3N_2$  diffused into it. The resistivity of each sample was then measured. Again, the conductivity of the high magnesium concentration film was higher than the low concentration. On the other hand, the conductivity of both the films containing magnesium was lower than that which contained no magnesium.

The reasons for the overall decrease in conductivity when magnesium is added are currently unclear. It could be that magnesium disrupts the diamond lattice which may inhibit the boron-controlled conductivity by creating defects. Alternatively, magnesium may reside at electrically inactive sites: magnesium could be anywhere – substitutional sites, interstitial sites or within the grain boundaries. It is possible that at low concentrations, the majority of magnesium may be at electrically inactive sites, resulting in the lower conductivity. As the concentration is increased, there is an increased probability that magnesium will exist at the ‘correct’ sites for allowing electrical conductivity or certain sites, such as the grain boundaries, may even become saturated and magnesium may be forced into less preferable but more electrically active sites. However, there is currently no evidence for this. Alternatively, magnesium may have a tendency to diffuse and form clusters which could be electrically inactive. This process may be easier when the concentration is lower but as the lattice becomes fuller or grain boundaries may become saturated, this diffusion may become more difficult, resulting in the increased conductivity. There is not yet enough evidence to be sure of the reasons for the observations in these experiments. Additional information (suggestions made in Chapter 5) would need to be carried out first.

The uncertainties associated with the measurements in these experiments were generally low but a more accurate test would be preferable, such as a 4-point probe method. In future studies, it would also be useful to determine the magnesium concentration at which the conductivity begins to increase. As well as this, Hall Effect measurements could be made to improve the accuracy of measurements and determine the carrier concentrations.

## Chapter 4 Conclusion

Magnesium was incorporated into a polycrystalline diamond film using an in-diffusion doping method with magnesium nitride as a source of magnesium. A suitable medium for the  $Mg_3N_2$  was found as chloroform with a small amount of polymer (polysorbate) which minimised oxidation and was sterically stable. It was found that the polymer was necessary to improve the distribution of particles in the suspension and reduce oxidation but if too much polymer was added, the magnesium diffusion into the film became hindered.

Magnesium was diffused into different types of diamond films – some were nitrogen-doped and some, boron-doped. A thin undoped capping layer was grown following the diffusion.

Characterisation by SEM shows that (100) square facets result when magnesium is diffused into a nitrogen-doped film and twinned facets are seen when magnesium is diffused into a boron-doped film. The edges of the facets are seen to be slightly ‘roughened’ compared to those when no magnesium is present. This ‘roughening’ effect is more pronounced for the nitrogen-doped films than the boron-doped films.

This incorporation of magnesium was confirmed by performing SIMS on the sample which showed a peak in the positive mode, assigned to the  $Mg^+$  ion, suggesting the presence of magnesium in the films. The broadening of the peak in both directions indicates the diffusion of magnesium both down into the first diamond layer and up into the second grown on top. The diffusion was approximately 200 nm in either direction which is greater than that of lithium.

The presence of the magnesium in the films was further implied by EDX measurements and a preliminary calculation of peak ratios suggested that a larger amount of  $Mg_3N_2$  deposited on top of the films resulted in a larger amount of magnesium was incorporated following diffusion. This characterisation technique is limited by its qualitative nature and inaccuracy in distinguishing the peaks as certain elements have peaks signals which are in close proximity and can interfere. Both EDX and SIMS have not provided information on the way in which Mg exists in the films – it is unclear from results so far whether magnesium resides on interstitial or substitutional sites or whether it lies mainly in the grain boundaries. In order to determine this, further experiments and characterisation techniques would need to be carried out such as XPS which would provide information on the chemical state of the magnesium.

It was also found that the flow rate of ammonia that was used when growing nitrogen-doped films, affected the incorporation of magnesium when diffusion was then performed. A flow rate of 0.75 sccm was too high for the magnesium to successfully diffuse into the magnesium. A flow rate of 0.2 sccm allowed the diffusion of magnesium into the film. However, varying the flow rate

of diborane, between 0.1 sccm and 0.5 sccm, when growing boron-doped films, did not have the same influence on the magnesium incorporation (0.5 sccm permitted magnesium incorporation).

Preliminary conductivity measurements showed that the presence of magnesium in nitrogen-doped films resulted in a high resistivity, as is the case when no magnesium is present.

Magnesium present in boron-doped diamond films seems to increase the resistivity compared to boron-doped films with no magnesium. However, a higher magnesium concentration resulted in a more conductive film than a low magnesium concentration.

Overall, it seem this successful incorporation of magnesium into a diamond film shows promise for generating n-type diamond that may demonstrate thermionic emission.

## Chapter 5 Future Work

### 5.1 X-Ray photoelectron spectroscopy (XPS)

From the results gathered in this study, it is unclear how the incorporated magnesium exists in the diamond film; it would be useful to have information indicating whether the magnesium occupies interstitial or substitutional sites or whether it is mainly found in the grain boundaries. These different possibilities could impact on the observations made. In some of these positions, the magnesium may be electrically inactive. Additionally, the grain boundaries may play an important role in the diffusion of lithium through the film (discussed in section 5.2 Role of the grain boundaries)

XPS provides information upon the chemical state of species, determining the local bonding environment and has an ability to differentiate between oxidation states of molecules. With this information, it should be possible to determine the way in which magnesium exists in the diamond film.

### 5.2 Role of the grain boundaries

If magnesium is situated in the grain boundaries of the film this could strongly influence the mobility of magnesium through the film. To measure this effect, magnesium could be diffused, as before, into a single crystal diamond film. This single crystal diamond film can be grown by HPHT techniques and will contain no grain boundaries. The sample can then undergo SIMS, as before. The width of the Mg peak indicates the distance the magnesium is diffusing through the film so by comparing the widths of the peaks from spectra of magnesium diffused into a polycrystalline film against magnesium diffused into a single crystal diamond film, the importance of grain boundaries upon diffusion processes can be inferred. It is likely, the grain boundaries increase the diffusion of magnesium and so a reduction in the width of the peak would be expected.

### 5.3 Diffusion conditions

In order to maximise the amount of magnesium incorporated into the diamond film, the diffusion conditions need to be optimized. Firstly, the time given for the magnesium to diffuse into the

diamond film in this study was 1 hour (plus 15 minutes as the capping layer was grown). It may be that a longer time period would allow the magnesium to incorporate more successfully into the film. Indeed, the magnesium may be able to diffuse further and this could be monitored by SIMS.

The amount of magnesium incorporated into the films may also be able to be increased. This could be done by increasing the concentration of  $Mg_3N_2$  solution or by increasing the amount of the solution that was deposited on top of the film. If a calibration sample was provided for SIMS, the depth profile could be given in terms of concentration and so it would be possible to find the concentration of magnesium throughout the film as well as determine if there was a saturation point.

## 5.4 Film quality

Raman spectroscopy can be used to determine the quality of the films. Quality is given as the ratio of graphitic ( $sp^2$ ) carbon to diamond ( $sp^3$ ) carbon. The diamond peak is at  $1333\text{cm}^{-1}$  and the graphitic peak is at  $1580\text{cm}^{-1}$ .

## 5.5 Test for thermionic emission

Tests could be carried out to identify the thermionic emission properties of the diamond films which have been diffused with magnesium.

## 5.6 Computational studies

Computational studies may be carried out to better predict the behaviour of magnesium in diamond; there is a great lack of work done on this topic. Computational studies similar to those done with lithium and sodium would provide information on the preferred site which magnesium would occupy in the lattice (substitutional or interstitial). Also a study to find the work function of diamond doped with magnesium would be useful in predicting the thermionic emission efficiency of this material and how magnesium affects the band structure

## Chapter 6 Acknowledgements

Special thanks to my supervisor Professor Paul May for his suggestions and expertise throughout the project. Also, to my second assessor Dr Neil Fox for helpful discussions. To Sarah Halliwell for assistance using the instruments, help obtaining the SIMS results and general guidance.

I would also like to thank the Electron Microscopy Unit (EMU) for use of the SEM and EDX equipment. Also, to the Interface Analysis Centre (IAC) for use of the SIMS equipment.

Additional thanks to the rest of the Bristol Diamond Group for their support.

## Chapter 7 Bibliography

- [1] P. W. May, *Philosophical Transactions of The Royal Society A*, vol. 358, no. 1766, pp. 473-495, 2000.
- [2] F. J. Ribeiro, P. Tangney, S. G. Louie and M. L. Cohen, *Physical Review B*, vol. 72, no. 214109, 2005.
- [3] A. Kruger, *Carbon Materials and Nanotechnology*, John Wiley and Sons, 2010.
- [4] P. Atkins and J. De Paula, *Physical Chemistry*, 9th ed., Oxford: Oxford University Press, 2010.
- [5] M. N. R. Ashfold, P. W. May, C. A. Rego and N. M. Everitt, *Chemical Society Reviews*, vol. 23, no. 1, pp. 21-30, 1994.
- [6] T. R. Anthony, *Vacuum*, vol. 41, no. 4-6, pp. 1356-1359, 1990.
- [7] F. P. Bundy, H. T. Hall, H. M. Strong and R. H. Wentorf, *Nature*, vol. 176, no. 4471, pp. 51-55, 1955.
- [8] P. W. Bridgman, *Scientific American*, vol. 193, no. 5, pp. 42-46, 1955.
- [9] *Synthetic Diamond*, New York: John Wiley & Sons, Inc, 1994, p. 10.
- [10] Y. Mokuno, A. Chayahara, H. Yamada and N. Tsubouchi, *Diamond and Related Materials*, vol. 18, no. 10, pp. 1258-1261, 2009.
- [11] J. C. Angus and C. C. Hayman, *Science*, vol. 241, no. 4868, pp. 913-921, 1988.
- [12] J. E. Butler, Y. A. Mankelewich, A. Cheesman, J. Ma and M. N. R. Ashfold, *Journal of Physics Condensed Matter*, vol. 21, no. 364201, 2009.
- [13] R. Haubner and B. Lux, *Diamond and Related Materials*, vol. 2, no. 9, pp. 1277-1294, 1993.
- [14] W. Banholzer, *Surface and Coatings Technology*, vol. 53, no. 1, pp. 1-12, 1992.
- [15] S. Matsumoto, Y. Sato, M. Kamo and N. Setaka, *Japanese Journal of Applied Physics*, vol. 21, pp. L183-L185, 1982.
- [16] C. Wolden, S. Mitra and K. K. Gleason, *Journal of Applied Physics*, vol. 72, no. 3750, 1992.
- [17] S. Matsumoto, Y. Sato, M. Tsutsumi and N. Setaka, *Journal of Materials Science*, vol. 17, no. 11, pp. 3106-3112, 1982.
- [18] S. Okoli, R. Haubner and B. Lux, *Surface and Coatings Technology*, vol. 47, no. 1-3, pp. 585-599, 1991.
- [19] P. Fauchais, A. Vardelle and A. Denoirjean, *Surface and Coatings Technology*, vol. 97, no. 1-3, pp. 66-78, 1997.
- [20] K. Suzuki, A. Sawabe, H. Yasuda and T. Inuzuka, *Applied Physics Letters*, vol. 50, no. 12, pp. 728-729, 1987.
- [21] N. Ohtake and M. Yoshikawa, *Journal of The Electrochemical Society*, vol. 137, no. 2, pp. 717-722, 1990.
- [22] K. Chen, M. Chuang, C. Murray Penney and W. F. Banholzer, *Journal of Applied Physics*, vol. 71, no. 1485, 1992.
- [23] E. Kondoh, T. Ohta, T. Mitomo and K. Ohtsuka, *Applied Physics Letters*, vol. 59, no. 4, p. 488, 1991.
- [24] I. Chen, *Journal of Applied Physics*, vol. 64, no. 7, p. 3742, 1988.
- [25] B. J. Waclawski, D. T. Pierce, N. Swanson and R. J. Celotta, *Journal of Vacuum Science and Technology*, vol. 21, no. 2, p. 368, 1982.
- [26] Y. Hirose and Y. Terasaw, *Japanese Journal of Applied Physics*, vol. 25, no. 6, pp. 519-521, 1986.
- [27] T. Kawato and K. I. Kondo, *Japanese Journal of Applied Physics*, vol. 26, no. 9, pp. 1429-1432, 1987.
- [28] D. M. Gruen, S. Liu, A. R. Krauss and J. Luo, *Applied Physics Letters*, vol. 64, no. 12, pp. 1502-1504, 1994.
- [29] H. I. D. E. Y. O. Okushi, “,” *Diamond and Related Materials*, vol. 10, no. 3, pp. 281-288, 2001.
- [30] X. Jiang, C. P. Klages, R. Zachai, M. Hartweg and H. J. Fusser, *Applied Physics Letters*, vol. 62, no. 26, pp. 3438-3440, 1993.
- [31] R. Locher, C. Wild, N. Herres, D. Behr and P. Koidl, *Applied Physics Letters*, vol. 65, no. 1, pp. 34-36, 1994.
- [32] M. W. Geis, N. N. Efremow and D. D. Rathman, *Journal of Vacuum Science and Technology A*, vol. 6, no. 3, pp. 1953-1954, 1988.
- [33] N. Fujimori, T. Imai and A. Doi, *Vacuum*, vol. 36, no. 1, pp. 99-102, 1986.
- [34] E. Brillas and C. A. Martinez-Huitle, *Synthetic Diamond Films*, Hoboken, New Jersey: John Wiley & Sons Inc., 2011.

- [35] R. F. Davis, Z. Sitar and B. E. Williams, *Materials Science and Engineering B*, vol. 1, no. 1, pp. 77-104, 1988.
- [36] R. Kalish, *Carbon*, vol. 37, pp. 781-785, 1999.
- [37] K. Thonke, *semiconductor Science and Technology*, vol. 18, no. 3, p. S20, 2003.
- [38] R. H. Wenotrf and H. P. Bovenkerk, *Journal of Chemical Physics*, vol. 36, p. 1987, 1962.
- [39] G. Braunstein and R. Kalish, *Journal of Applied Physics*, vol. 54, p. 2106, 1983.
- [40] C. Johnston, A. Crossley, M. Werner and P. R. Chalker, *Properties, Growth and Applications of Diamond*, vol. 26, INSPEC: London, 2001, pp. 337-347.
- [41] J. P. Goss and P. R. Briddon, *Physical Review B*, vol. 73, no. 8, p. 085204, 2006.
- [42] C. Uzan-Saguy, R. Kalish, R. Walker, D. N. Jamieson and S. Praver, *Diamond and Related Materials*, vol. 7, no. 10, pp. 1429-1432, 1998.
- [43] J. Chevallier, B. Theys, A. Lussou and C. Grattapain, *Physical Review B*, vol. 58, pp. 7966-7969, 1998.
- [44] J. Mort, D. Kuhman, M. Machonkin, M. Morgan, F. Jansen, K. Okumura, Y. LeGrice and R. J. Nemanich, *Applied Physics Letters*, vol. 55, p. 1121, 1989.
- [45] A. T. Collins and A. W. S. Williams, *Journal of Physics C: Solid State Physics*, vol. 4, no. 13, p. 1789, 1971.
- [46] R. M. Chrenko, *Physics Review B*, vol. 7, pp. 4560-4567, 1973.
- [47] H. B. Dyer, F. A. Raal, L. Du Preez and J. H. N. Loubser, *Philosophical Magazine*, vol. 11, no. 112, pp. 763-774, 1965.
- [48] J. Robertson and C. A. Davis, *Diamond and Related Materials*, vol. 4, no. 4, pp. 441-444, 1995.
- [49] S. A. Kajihara, A. Antonielli and J. Bernholc, *Physical Review Letters*, vol. 66, no. 15, 1991.
- [50] R. Kalish, *Diamond and Related Materials*, vol. 10, no. 9, pp. 1749-1755, 2001.
- [51] B. B. Li, M. C. Tosin, A. C. Peterlevitz and V. Baranauskas, *Applied Physics Letters*, vol. 73, no. 6, pp. 812-814, 1998.
- [52] R. G. Farrer, *Solid State Communications*, vol. 7, pp. 685-688, 1969.
- [53] G. B. Bachelet, G. A. Baraff and M. Schluter, *Physical Review B*, vol. 24, no. 8, p. 4736, 1981.
- [54] S. Jin and T. D. Moustakas, *Applied Physics Letters*, vol. 65, no. 4, p. 403, 1995.
- [55] Y. Bar-Yam and T. D. Moustakas, *Nature*, vol. 342, p. 786, 1989.
- [56] G. L. Pearson and J. Bardeen, *Physical Review*, vol. 75, no. 5, p. 865, 1949.
- [57] C. Yamanouchi, K. Mizuguchi and W. Sasaki, *Journal of the Physical Society of Japan*, vol. 22, p. 859, 1967.
- [58] S. Koizumi, M. Kamo, Y. Sato, H. Ozaki and T. Inuzuka, *Applied Physics Letters*, vol. 71, no. 8, p. 1065, 1997.
- [59] E. Gheeraert, N. Casanova, A. Tajani, A. Deneuve, E. Bustarret, J. A. Garnido, C. E. Nebel and M. Stutzmann, *Diamond and Related Materials*, vol. 11, no. 3, p. 289, 2002.
- [60] I. Sakaguchi, N. Mikka, Y. Kichuchi, E. Yasu, H. Haneda, T. Suzuki and T. Ando, *Physical Review B*, vol. 60, no. 4, p. R2139, 1999.
- [61] R. Kalish, A. Reznik, C. Uzan-Saguy and C. Cytermann, *Applied Physics Letters*, vol. 76, no. 6, p. 757, 2000.
- [62] E. B. Lombardi and A. Mainwood, *Diamond and Related Materials*, vol. 7, no. 7, p. 1349, 2008.
- [63] J. F. Prins, *Physical Review B*, vol. 61, no. 11, p. 7191, 2000.
- [64] M. Rostle, K. Bharuth-Rum, H. Quintel, C. Ronning, H. Hofsass and S. G. Jahn, *Applied Physics Letters*, vol. 66, no. 20, p. 2733, 1995.
- [65] J. Bernholc, A. Antonelli, T. M. Del-Sole, Y. Bar-Yam and S. T. Pantelides, *Physical Review Letters*, vol. 61, no. 23, p. 2689, 1988.
- [66] C. Uzan-Saguy, C. Cytermann, B. Fizgeer, V. Richter and R. Brenner, *Physica Status Solidi A*, vol. 193, no. 3, p. 508, 2002.
- [67] E. B. Lombardi, A. Mainwood and K. Osuch, *Physical Review B*, vol. 75, no. 15, p. 155203, 2007.
- [68] M. Z. Othman, P. W. May, N. A. Fox and P. J. Heard, *Diamond & Related Materials*, vol. 44, pp. 1-7, 2014.
- [69] T. H. Borst and O. Weis, *Diamond and Related Materials*, vol. 4, no. 7, p. 948, 1995.
- [70] D. Saada, J. Adler and R. Kalish, *Applied Physics Letters*, vol. 77, no. 6, p. 878, 2000.
- [71] S. A. Kajihara, A. Antonelli and J. Bernholc, *Physica B: Condensed Matter*, vol. 185, no. 1-4, pp. 144-149, 1993.
- [72] G. Popovici and M. A. Prelas, *Diamond and Related Materials*, vol. 4, pp. 1305-1310, 1995.

- [73] G. Popovici, R. G. Wilson, T. Sung, M. A. Prelas and S. Khasawinah, *Journal of Applied Physics*, vol. 77, no. 10, p. 5103, 1995.
- [74] J. P. Goss, R. J. Eyre and P. R. Briddon, *Physica Status Solidi b*, vol. 245, no. 9, pp. 1679-1700, 2008.
- [75] K. Okumura, J. Mort and M. Machonkin, *Applied Physics Letters*, vol. 57, no. 18, p. 1907, 1990.
- [76] J. F. Prins, *Diamond and Related Materials*, vol. 4, pp. 580-585, 1995.
- [77] R. Kalish, C. Uzan-Saguy, A. Samoiloff, R. Locher and P. Koidl, *Applied Physics Letters*, vol. 64, no. 19, pp. 2532-2534, 1994.
- [78] B. V. Spitsyn, L. L. Bouilov and B. V. Derjaguin, *Journal of Crystal Growth*, vol. 52, pp. 219-226, 1981.
- [79] J. R. Flemish, S. N. Schauer and R. Wittstruck, *Diamond and Related Materials*, vol. 3, pp. 672-676, 1994.
- [80] S. Koizumi, T. Teraji and H. Kanda, *Diamond and Related Materials*, vol. 9, pp. 935-940, 2000.
- [81] M. Panizza and G. Cerisola, *Electrochimica Acta*, vol. 51, no. 2, pp. 191-199, 2005.
- [82] H. B. Martin, A. Argottia, U. Landau, A. B. Anderson and J. C. Angus, *Journal of the Electrochemical Society*, vol. 143, no. 6, 1996.
- [83] C. Reuben, E. Galun, H. Cohen, R. Tenne, R. Kalish, Y. Muraki, K. Hashimoto, A. Fujishima, J. M. Butler and C. Levy-Clement, *Journal of Electroanalytical Chemistry*, vol. 396, no. 1, pp. 233-239, 1995.
- [84] J. C. Male and J. R. Prior, *Nature*, vol. 186, pp. 1037-1038, 1960.
- [85] K. Okana, H. Kiyota, T. Iwasaki, T. Kurosu, M. Iida and T. Nakamura, *Applied Physics Letters*, vol. 58, p. 840, 1991.
- [86] S. Koizumi, K. Watanabe, M. Hasegawa and H. Kanda, *Science*, vol. 292, no. 5223, pp. 1899-1901, 2001.
- [87] K. Shenai, R. S. Scott and B. B. Jayant, *IEEE Transactions on Electron Devices*, vol. 36, no. 9, pp. 1811-1823, 1989.
- [88] T. H. Borst, S. Strobel and O. Weis, *Applied Physics Letters*, vol. 67, p. 2651, 1995.
- [89] K. P. McKenna and A. L. Shluger, *Nature Materials*, vol. 7, pp. 859-862, 2008.
- [90] C. Bandis and B. B. Pate, *Physical Review B*, vol. 52, p. 12056, 1995.
- [91] F. A. Koeck, R. J. Nemanich, A. Lazea and K. Haenen, *Diamond & Related Materials*, vol. 18, pp. 789-791, 2009.
- [92] F. A. Koeck, J. M. Garguilo and R. J. Nemanich, *Diamond & Related Materials*, vol. 13, pp. 2052-2055, 2004.
- [93] J. van der Weide, z. zhang, P. K. Baumann, M. G. Wensell, J. Bernholc and R. J. Nemanich, *Physical Review B*, vol. 50, p. 5803, 1994.
- [94] K. M. O'Donnell, T. L. Martin, N. A. Fox and D. Cherns, *Physical Review B*, vol. 82, p. 115303, 2010.
- [95] M. Suzuki, T. Ono, N. Sakuma and T. Sakai, *Diamond & Related Materials*, vol. 18, no. 10, pp. 1274-1277, 2009.
- [96] <http://www.chm.bris.ac.uk/pt/diamond/thermionic.htm>.
- [97] S. L. Flegler, J. W. Heckman and L. K. K., *Scanning and Transmission Electron Microscopy: An Introduction*, New York: W H Freeman, 1993.
- [98] B. R. Stoner, B. E. Williams, S. D. Wolter, K. Nishimura and J. T. Glass, *Journal of Materials Research*, vol. 7, no. 2, pp. 257-260, 1992.
- [99] P. Atkins and J. De Paula, *Physical Chemistry*, 9th ed., Oxford: Oxford Univeristy Press, 2010, p. 260.
- [100] H. Seiler, *Journal of Applied Physics*, vol. 54, no. R1, 1983.
- [101] J. C. Vickerman and I. S. Gilmore, *Surface Analysis: The Principle Techniques*, 2nd ed., Chichester: John Wiley & Sons, 2009.
- [102] H. Spicka, M. Griesser, H. Hutter, M. Grasserbauer, S. Bohr, R. Haubner and B. Lux, *Diamond and Related Materials*, vol. 5, pp. 383-387, 1996.
- [103] S. Hofman, *Philosophical Transactions of The Royal Society*, vol. A362, pp. 55-75, 2004.
- [104] D. McPhail, *Journal of Materials Science*, vol. 41, no. 3, pp. 873-903, 2006.
- [105] R. Ekman, J. Silberring, A. M. Westman-Brinkmalm and A. Kraj, *Mass Spectrometry: Instrumentation, Interpretation and Applications*, Hoboken: John Wiley & Sons, 2009.
- [106] J. Barker, *Mass Spectrometry*, 2nd ed., Chichester: John Wiley & Sons, 1999, p. 345.
- [107] D. K. Schroder, *Semiconductor Material and Devices*, 3rd ed., Hoboken: John Wiley & Sons, 2006.

- [108] S. Amelinckx, D. van Dyck, J. van Landuyt and G. van Tendeloo, *Handbook of Microscopy Methods II*, Weinheim: VCH, 1997.
- [109] P. J. Goodhew, J. Humphreys and R. Beanland, *Electron Microscopy and Analysis*, 3rd ed., New York: Taylor & Francis, 2001.
- [110] J. A. Chandler, *X-Ray Microanalysis in the Electron Microscope*, Amsterdam: North-Holland, 1977.
- [111] P. W. May, P. R. Burridge, C. A. Rego, R. S. Tsang, M. N. R. Ashfold, K. N. Rosser, R. E. Tanner, D. Cherns and R. Vincent, *Diamond & Related Materials*, vol. 5, no. 3-5, pp. 354-358, 1996.
- [112] K. Ushizawa, K. Watanabe, T. Ando, I. Sakaguchi, M. Nishitani-Gamo, Y. Sato and H. Kanda, *Diamond & Related Materials*, vol. 7, pp. 1719-1722, 1998.
- [113] S. Yugo, T. Kanai, T. Kimura and T. Muto, *Applied Physics Letters*, vol. 58, no. 1036, 1991.

## Chapter 8 Appendix

### Resistivity measurements

#### Experiment 3

Sample	Resistivity ( $\Omega$ )			
	Test 1	2	3	4
Nitrogen-doped + low magnesium concentration	>20 M $\Omega$			
Nitrogen-doped + high magnesium concentration	>20 M $\Omega$			
Boron-doped + low magnesium concentration	1930 $\Omega$	1920 $\Omega$	1945 $\Omega$	1912 $\Omega$
Boron-doped + high magnesium concentration	1350 $\Omega$	1400 $\Omega$	1342 $\Omega$	1326 $\Omega$

#### Experiment 4

Sample	Diborane flow rate (sccm)	Mg <sub>3</sub> N <sub>2</sub>	Resistivity ( $\Omega$ )				
			Test 1	2	3	4	5
A	0.5	None	10.6	10	11	15.1	16.8
B	0.5	Low concentration	880	888	887	875	878
C	0.5	High concentration	314	314	313	313	314